



The author(s) shown below used Federal funding provided by the U.S. Department of Justice to prepare the following resource:

Document Title: Optimization and Statistical Testing of Experimental and Computer Methodologies for Evaluation of the LIT-MIA Thermal Imaging Method for Recovery of Defaced Serial Numbers

Author(s): Rene Rodriguez, Anit Gurung, Lisa Lau, John Kalivas

Document Number: 304649

Date Received: April 2022

Award Number: 2017-DN-BX-0173

This resource has not been published by the U.S. Department of Justice. This resource is being made publicly available through the Office of Justice Programs' National Criminal Justice Reference Service.

Opinions or points of view expressed are those of the author(s) and do not necessarily reflect the official position or policies of the U.S. Department of Justice.

Final Report on the Project "Optimization and Statistical Testing of Experimental and Computer Methodologies for Evaluation of the LIT-MIA Thermal Imaging Method for Recovery of Defaced Serial Numbers "

Award Number: 2017-DN-BX-0173

Author(s): Rene Rodriguez, Anit Gurung, Lisa Lau, John Kalivas

Abstract

The overall problem under investigation was optimization of the recovery of serial numbers from metallic objects such as firearms or automobile engines using non-destructive techniques based on the localized changes in the thermal conductivity of a substance known as thermal infrared imaging or infrared thermography coupled with sophisticated multivariate image analysis (MIA) techniques. The thermal imaging equipment and techniques used for this work were largely based on our previous proposal "Infrared Thermal Imaging for Use in Restoration of Defaced Serial Numbers", Award Number 2013-R2-CX-K012. One significant change was the replacement of the laser used for pulsed heating of the sample and replacement of the homebuilt pulse timing box with a commercially available system. Other variations attempted here included increasing the layers of black paint or black electrical tape instead of 1 layer of paint to cover the defaced area and allow heating of the sample by the laser. The use of the electrical tape proved helpful in determining the frequencies that would be best suitable for recovery of the defaced numbers and the frequency depended on the depth to which the number was defaced.

With regard to processing and the use of multivariate image processing methods, in the 2013 studies, direct library comparison of the Zernike and Pseudo Zernicke Moments of the numbers in the Number Library to those of the score images derived from Principal Component Analysis (PCA) of the phase or amplitude images derived from the infrared imaging of the defaced samples. In these studies, the use of Classification Techniques (classifiers) which involve a comparison of a vector to a spatial domain defined by a class were also investigated as a comparison method for computer identification of the identity of the defaced number. The library was also expanded to include letters in addition to the numbers, and several more fonts were included as well. The library also included "dilated" and "thinned" sets of the characters in an attempt to account for possible deformations in the defaced images.

A major focus of these studies was to evaluate the ability of our thermal imaging technique to recover the defaced serial numbers through "blind" or "black box" studies. In these studies, the location of the numbers is largely unknown. This differs from all of the samples used in our 2013 studies as the location of the defaced numbers was known exactly or to a fairly high degree of certainty. To accomplish our "black box" studies, we participated in the CTS Forensic Services serial number recovery test in July 2019 (Test No. 19-5251) and also in "black box studies with our collaborators at the Idaho State Police Forensic Services Lab in Coeur d'Alene Idaho. The results were: 1) we were unable to identify the six defaced serial numbers correctly when we participated in the CTS Forensic Services studies. 2) In our blind studies that included subsequent recovery by the Idaho State Police, we identified 8 out of 42 characters correctly, and the police lab identified 29 of the 42 characters correctly. The 42 characters were stamped in 3 different types of metals: aluminum, stainless steel, and rolled steel, 7 characters in

each type of metal at two different depth of defacing. The 8 characters we identified correctly were also identified correctly by the Idaho State Police. Again, in both the samples for the black box studies with the ISP and the CTS Forensic samples the locations of the numbers were largely unknown to any degree of certainty. Dividing the number of characters identified correctly by the total number of defaced characters from all the samples, the success rate in correctly identifying a defaced serial number by thermal imaging is about 19% using the thermal imaging method and 69% by the Idaho State Police Lab using wet chemical methods. In these blind studies the exact location of the number is unknown. If the location is known, based on the results from our last grant, the success rate is somewhat higher.

Table of Contents

Abstract	1
List of Figures	3
List of Tables	8
Executive Summary	9
I. Introduction	11
II. Work Performed	13
II A. Surface Prep and Recovery Depth	14
II. B. Score Image Contribution	31
IIC. Similarity Merits	48
Dilation Effects	49
Effect of Allowing for Rotational Variance	54
IID. Libraries and Computer Matching Algorithms	57
III. Black-Box” or “Blind” Studies Results	59
IV. Summary	66
V. References	69
VI. Dissemination of Research Findings	69
Appendix 1 Similarity Merits	71

List of Figures

Figure 1. Original graded sample, as received from the company.	14
Figure 2. Graded Sample after being defaced.	14
Figure 3. PCA image most representative of the original number for samples prepared with one coating of black paint.	15
Figure 4. PCA image most representative of the original number for samples prepared with two coatings of black paint.	15
Figure 5. Thermal imaging with no external heating of serial numbers, 2 (non-defaced) and 6 (partially defaced), on a stainless steel: a) without a black electric tape and b) black electrical tape on the surface	16
Figure 6. Thermal, Phase (ϕ), and Amplitude (A) images for undefaced 2 at each 7 different lock-in frequencies (0.125, 0.25, 0.5, 1, 2, 4 and 8Hz)	18
Figure 7. Thermal, Phase (ϕ) and Amplitude (A) images for partially defaced six at each 7 different lock-in frequencies (0.125, 0.25, 0.5, 1, 2, 4 and 8Hz)	19
Figure 8. Phase image of the 22 cycle average from the 2nd machined step of the defaced aluminum stepped sample.	21
Figure 9. Score plots 2-12 in the region where the defaced 8 should be located.	22
Figure 10. Score plots of the aluminum step sample from the area where the defaced 2 on the 2nd step should be present in the image	23
Figure 11. Phase image of the 22 cycle average from the 2nd machined step of the defaced steel stepped sample.	24
Figure 12. Left - Black and white image from the amplitude image in score plot 10 visually the best match for the defaced 8. Right – Black and white image from the amplitude image of score plot 9 in the area of the defaced 6.	25
Figure 13. Amplitude image of steps 2 and 3 from the stainless steel sample.	26
Figure 14. Picture of defaced CTS zinc test sample after sanding and applying black paint.	27
Figure 15. Photo of initial sample orientation chosen to view the characters. Blue rectangle shows approximate camera view of sample for this movie.	27
Figure 16. Phase diagram of full width of camera view for 8 frames per cycle and 22 cycles averaged. Box shows possible disturbances in the pattern that could be a number “2”	28
Figure 17. Score plots 5, 6, 7, and 8 derived from one movie of 8 frames per cycle and 22 cycles averaged. Score plot 6 looks very much like number 2.	29
Figure 18. Fusion sums from library match to score images 1-15 for 4th character.	29

Figure 19. Score image PC4 derived from phase images of cycles 1-15 and corresponding character determination by fusion rules. (lowest sum of rankings is best fit)	31
Figure 20. Score image PC4 derived from phase images of cycles 1-20 and corresponding character determination by fusion rules. (lowest sum of rankings is best fit)	32
Figure 21. Score images PC1-15 derived from phase images of cycles 1-60 and corresponding character determination by fusion rules. (lowest sum of rankings is best fit)	32
Figure 22. Score images PC1-15 derived from phase images of cycles 6-60 and corresponding character determination by fusion rules.	32
Figure 23. Score images PC1-15 derived from phase images of cycles 11-60 and corresponding character determination by fusion rules.	33
Figure 24. Score images PC1-15 derived from phase images of cycles 16-60 and corresponding character determination by fusion rules.	33
Figure 25. Score images PC1-15 derived from phase images of cycles 21-60 and corresponding character determination by fusion rules.	33
Figure 26. Score images PC1-15 derived from phase images of cycles 25-60 and corresponding character determination by fusion rules.	33
Figure 27. Score images PC1-15 derived from phase images of cycles 31-60 and corresponding character determination by fusion rules.	34
Figure 28. Score images PC1-15 derived from phase images of cycles 35-60 and corresponding character determination by fusion rules.	34
Figure 29. Score images PC1-15 derived from phase images of cycles 40-60 and corresponding character determination by fusion rules.	34
Figure 30. Score images PC1-15 derived from phase images of cycles 46-60 and corresponding character determination by fusion rules.	35
Figure 31. Score images PC1-10 derived from phase images of cycles 51-60 and corresponding character determination by fusion rules.	35
Figure 32. Score images PC1-5 derived from phase images of cycles 56-60 and corresponding character determination by fusion rules.	35
Figure 33. Temporal Profile - Temperature (66.5-70.0 °C) vs Lock-in Cycle Number for each of the 61 heating cycles for Defaced 6.	36
Figure 34. Score images PC1-15 derived from phase images of cycles 1-15 and corresponding character determination by fusion rules.	37
Figure 35. Score images PC1-15 derived from phase images of cycles 1-60 and corresponding character determination by fusion rules.	37

Figure 36. Score images PC1-15 derived from phase images of cycles 21-60 and corresponding character determination by fusion rules.	38
Figure 37. Score images PC1-15 derived from phase images of cycles 46-60 and corresponding character determination by fusion rules.	38
Figure 38. Score images PC1-15 derived from phase images of cycles 50-60 and corresponding character determination by fusion rules.	38
Figure 39. Score images PC1-15 derived from phase images of cycles 56-60 and corresponding character determination by fusion rules.	38
Figure 40. Binary image processed from phase shift at optimal lock-in frequency (1Hz) for undefaced two (left) and partly defaced six (right) with two replicates: a) original analysis, b) replicate.	40
Figure 41. Classification using PCA and PLS-DA.	42
Figure 42. An example of kNN classification.	42
Figure 43. Fusion Classification input matrix and sum fusion value (undefaced 2- first replicate) with RM of a specific proportion (35%) and tuning parameter window size of forty-five.	44
Figure 44. Bar plot of Classification Sum Fusion for first replicate of undefaced two with PZM at 50% dilation of the phase image. The magenta color bar represents the lowest sum fusion value (lowest rank).	45
Figure 45. Bar plot of Classification Sum Fusion for partially defaced six and varying object percentage at 50% dilation of the phase image. The magenta color bars represent the lowest sum fusion value (lowest rank).	45
Figure 46. Picture of Shotgun before and after the model number was defaced.	46
Figure 47. Phase and Enhanced Binary images of defaced 1 on the shotgun barrel. Also shown is the Sum Fusion for identifying the character using the Classification comparison method.	46
Figure 48. Phase and Enhanced Binary images of defaced 2 on the shotgun barrel. Also shown is the Sum Fusion for identifying the character using the Classification comparison method.	47
Figure 49. Picture of Forceps before and after the serial number was defaced.	47
Figure 50. Phase and Enhanced Binary images of defaced 3 on the Forceps (Needle Holder). Also shown is the Sum Fusion for identifying the character using the Classification comparison method.	47
Figure 51. Phase and Enhanced Binary images of defaced 4 on the Forceps (Needle Holder). Also shown is the Sum Fusion for identifying the character using the Classification comparison method.	48

Figure 52. Score Image of a Defaced 2 compared with a Segoe 2 from the number library.	49
Figure 53. Comparison of the undilated score image to multifont image library.	49
Figure 54. 201 x 111 Pixel Dilated Score Image for comparison with Segoe library font image	50
Figure 55. Successive Dilation of the Score image for comparison with the number 2 from the Segoe font. Identification of the defaced image as a number 2 is much improved.	50
Figure 56. An example of morphological operations performed on binary image converged to different object area percentage a) 35% b) 50% and c) 65%	51
Figure 57. Bar plot of Sum Fusion for defaced 1 on the shotgun barrel with dilation by a) 35%, b) 50% and c) 65%. The magenta color bars represent the lowest sum fusion value.	52
Figure 58. Bar plot of Sum Fusion for defaced 2 on the shotgun barrel with dilation by a) 35%, b) 50% and c) 65%. The magenta color bars represent the lowest sum fusion value.	52
Figure 59. Bar plot of Sum Fusion for defaced 3 on the forceps with dilation by a) 35%, b) 50% and c) 65%. The magenta color bars represent the lowest sum fusion value.	53
Figure 60. Bar plot of Sum Fusion for defaced 4 on the forceps with dilation by a) 35%, b) 50% and c) 65%. The magenta color bars represent the lowest sum fusion value.	53
Figure 61. Score image of the Defaced 2 and the score image rotated by 180°	54
Figure 62. Score image of the Defaced 6 and the score image rotated by 180°	54
Figure 63. Ranking for Defaced 6 w/Dilation and the rotationally variant RM moments.	55
Figure 64. Ranking for Defaced 6 w/Dilation and the rotationally variant RM moments.	55
Figure 65. Ranking for Defaced 5 w/Dilation and the rotationally variant RM moments.	56
Figure 66. Ranking for Defaced 5 w/Dilation and the rotationally invariant PZM moments.	56
Figure 67. Bar plot of Sum Fusion for first replicate of undefaced 2 with RM and varying object percentage a) 35%, b) 50% and c) 65%. The magenta color bar represents the lowest sum fusion value.	56
Figure 68. Bar plot of Sum Fusion for first replicate of undefaced 2 with PZM and varying object percentage a) 35%, b) 50% and c) 65%. The magenta color bar represents the lowest sum fusion value.	57
Figure 69. Capability of individual fonts to identify the defaced number as a 6. (Note that the Dark blue color indicates the best fit and red is the worst fit.) Here the Times New Roman (italics), Gungsoh (Normal), and Arial Black (italics) indicated that the best fit was a number 6.	58
Figure 70. Capability of individual fonts to identify the defaced number as a 5. (Note that the Dark blue color indicates the best fit and red is the worst fit.) Here the Gungsoh (Normal) font indicated that the best fit was a number 5.	58

Figure 71. Field Defined for Defaced serial number divided into sections labeled T U V W X Y and Z.	61
Figure 72. Score plots derived from thermal images of Section T on defaced sample B1.	62
Figure 73. Sum of Fusion Values for each Score Image (s1, s2, s3 ...), for Character Position T, from Library Match of the score images and the overall sum of the fusion values. Minimal sum indicates the best match.	62
Figure 74. Score images 5 and 6 for Character T. Score image 5 looks mostly like a 7 and Score Image 6 looks mostly like an 8.	63
Figure 75. Score plots derived from thermal images of Section Z on defaced sample B1.	63
Figure 76. Sum of Fusion Values for each Score Image (s1, s2, s3 ...), for Character Position Z, from Library Match of the score images and the overall sum of the fusion values. Minimal sum indicates the best match.	64
Figure 77. Score images 6 and 7 for Character Z. Score image 6 looks mostly like a 6 and Score Image 7 looks mostly like an 8.	64

List of Tables

Table 1. Tabulation of Lock-in frequencies and the respective frame rate	17
Table 2. Results from the Majority Vote library matching for defaced 8 on 2 nd Step	22
Table 3. Results from the Majority Vote library matching for defaced 2 on 2 nd Step.	24
Table 4. Results from the Majority Vote library matching for the defaced 8 and defaced 6 on the stepped stainless steel sample.	25
Table 5. List of the Sample Material, Deface Depth and Serial Number for 2 nd Study	60
Table 6. Comparison of the Serial Number Recovery Results from the Thermal Imaging and Wet Chemical Method	65

Executive Summary

The purpose of this research was to attempt to optimize our thermal imaging coupled with multivariate image analysis method and to determine the success rate of the method by performing blind studies with defaced samples provided the CTS Forensic Testing service and also with stamped metals which were defaced by an independent machinist without our knowledge of the identity of the numbers or their placement on the surface of the sample.

The optimization of the thermal imaging required a re-examination of some of the experimental parameters: the temperature of the defaced sample, the power of the laser, the polishing of the sample, the method used to blacken the defaced sample, and the best lock-in frequency to be used to make the phase images, and also a re-examination of the multivariate image methods that used to process the lock-in thermographic images and to compare them with the images of various fonts of numbers and letters collected in an image library.

With regard to the reassessment of the experimental parameters, in our old studies we were heating the defaced samples up to $\sim 70^{\circ}\text{C}$ before the pulsed laser hit the sample and created the phase and amplitude images. This preheating was performed in an effort to discriminate the defaced sample from the background which was at room temperature. In these studies, we found that if the correct lock-in frequencies were used, the need to preheat the defaced samples was minimized. In fact, the pulsed laser hitting the samples when they were just at room temperature, resulted in a larger temperature swing in the sample, and likely increased the reliability of construction of the phase images and amplitude images of the defaced samples.

Since room temperatures could be used for the defaced samples, the laser power at the sample required to get a similar temperature swing was lower. A temperature swing of about 1°C seemed adequate. The temperature swing achieved depends both on the power of the laser and also the pulse frequency. As in our last studies, we found that the optimal laser pulse and lock-in frequency depended on both the preparation of the surface: the thickness of the paint (or for these studies the black tape) and also on the depth to which the sample was defaced. Thus the laser power should be high enough to provide approximately a 1°C temperature swing in the sample if possible. As mentioned, the thickness of the black paint or black tape plays a role in finding the optimal lock-in frequency and therefore must be taken into account when selecting the optimal experimental parameters. In practice, using the black tape as the heat absorbing surface, the optimal parameters might best be found by first examining a metal with an undefaced number stamped on it, and determine the temperature swing at several pulse frequencies likely to be useful for that type of metal sample and deface depth if there is something known about it.

With regard to optimization of the image processing and subsequent analysis, in our previous grant we employed Principal Component Analysis of the phase and amplitude images to generate score images. Moments from Zernicke and Pseudo Zernicke polynomials fitted to the score images were determined and these were then matched with similar moments from library images of number fonts using several. Then similarity merits comparing score image and library image moments were generated, and a fusion of these rules provided for a largely

computer-based identification of the serial numbers. In these studies we found that using the radial part of the Zernicke and pseudo Zernicke polynomials gave moments that were sensitive to the orientation of the number, “rotationally variant”, whereas the use of the moments from the entire Zernicke polynomial that were insensitive to the rotational orientation. Use of the radial polynomial, the rotationally variant polynomial, increased the success at matching the score images to the library images.

We also investigated the use of a different method to compare the processed thermal images of the defaced serial numbers with the library of numbers. Our original method employed a direct comparison of the Zernicke and Pseudo Zernicke Moments images of the Microsoft Word fonts to those of the score images derived from Principal Component Analysis (PCA) of the phase or amplitude images of the infrared images of the defaced samples. This was done using several measures of merit and then employing a set of fusion rules. In these new studies, Classification Techniques (classifiers) which involve a comparison of a vector to a spatial domain defined by a class were investigated as a comparison method for computer identification of the defaced number. These studies were performed by applying the Classification Technique directly to the phase images, not the score images. The library was also expanded to include both letters and numbers, and several more fonts were included as well. The library also included “expanded” and “thinned” sets of the characters in an attempt to account for possible deformations in the defaced images. Use of the classification techniques for computer aided serial number determination from phase images of samples used in our previous studies: 1) the defaced graded sample, 2) the defaced numbers on a shotgun barrel, and on 3) the defaced laser engraved serial number on the forceps correctly identified the defaced serial number and compared favorably with our previous method which used the score images. Note that in each of these samples, the position of the defaced numbers was approximately known.

The most significant results from the current studies involved using the thermal imaging techniques to perform “black-box” or “blind” defaced serial number recovery studies. Three of these studies were performed in conjunction with our law enforcement collaborators. Overall there were a total of 4 blind test samples. One was obtained from CTS Forensic Testing Service as part of the National Examination (the results were provided by the testing service) and there were 3 metals samples (aluminum, stainless steel, and rolled steel, defaced by the independent machinist with subsequent testing of the same samples by our collaborators at the Idaho State Police Lab in Coeur d’Alene Idaho. The subsequent testing was possible because the thermal imaging method is a non-destructive method. Due to onset of the pandemic, our collaborator at the Utah State Lab did not participate and only the Idaho State Police Lab participated in the studies with us. The results were: 1) we were unable to identify the six defaced serial numbers correctly when we participated in the CTS Forensic Services studies; 2) in our blind studies that included subsequent recovery by the Idaho State Police, we identified 8 out of 42 characters correctly, and the police lab identified 29 of the 42 characters correctly. The 42 characters were stamped in 3 different types of metals: aluminum, stainless steel, and rolled steel, 7 characters in each type of metal. The 8 characters we identified correctly were also

identified correctly by the Idaho State Police. Again, in both the samples for the black box studies with the ISP and the CTS Forensic samples the locations of the numbers were largely unknown to any degree of certainty. From the Black-Box Studies, dividing the number of characters identified correctly by the total number of defaced characters from all the samples, the success rate in correctly identifying a defaced serial number by thermal imaging is about 19% if the exact location of the number is unknown. If the location is known, based on the results from our last grant, the success rate is likely somewhat higher.

I. INTRODUCTION

The overall purpose of the research project titled " Optimization and Statistical Testing of Experimental and Computer Methodologies for Evaluation of the LIT-MIA Thermal Imaging Method for Recovery of Defaced Serial Numbers" was to attempt to optimize the use Infrared Imaging techniques complimented with Multivariate Image Processing to recover defaced serial numbers. The physical basis of this number recovery method relies on the ability of the infrared (IR) camera to discern differences in the heat flow, i.e. thermal conductivities, of the metal in areas where the metal is relatively pristine as compared to areas where the metal was deformed by stamping or engraving a serial number into the metal. As addressed in the research proposal, the following research questions and hypotheses were to be addressed by this research.

The specific aims for this proposal were

1. Determine limits on the depth of recovery as a function of surface preparation and on the temperature swings achieved with the pulses. **(Surface Prep and Recovery Depth)**
2. Study how to best streamline the computer multivariate processing methodology by examining whether each PCA score image contributes more, little, or nothing to the recovery. **(Score Image Contribution)**
3. Determine if each similarity measure and type of similarity measure contributes significantly to providing a reliable matching of the recovered serial number to the library using cross validation methods, develop a set of "fusion rules" to combine these similarity measures based on optimizing the reliability of the recovery. **(Best Use of Similarity Measures)**
4. Study the amount and types of number libraries to include, for the computer-based matching algorithms. **(Libraries and Computerized Matching Algorithms)**
5. Participate in "black box" studies with our law enforcement partners aimed at measuring the validity of the method with regard to it reproducibility and reliability. In part this should involve a comparison of the LIT-MIA infrared thermal imaging technique to conventional serial number recovery methods. **(“Black-Box” or “Blind” Studies Results)**

Results from studies performed for each of the five specific aims will be described in separate sections of this final report followed by a summary section.

As this is related to the findings of a previous grant, a summary of the pertinent information from the previous grant is given. Use of lock-in thermography (LIT) provided the best results of the methods attempted, and the studies here used only the lock-in thermography technique. The LIT instrument was constructed from an ~2 Watt pulsed laser heating source

chopped at a frequency between 0.025 Hz and 10 Hz. The pulsed laser source was directed onto a heated, polished, and painted sample, imaged with a FLIR SC6700 model infrared camera after first passing through a “top hat” beam flattening optic. This LIT setup provided the capacity needed to construct phase images of the defaced samples. In the previous grant, the lock-in experiments required taking multiple images at equal spaced intervals after the heating source pulse and before the next pulse began. Mathematical manipulation of the multiple images provided for both magnitude and phase images of the defaced area on the metal. The phase images are images where background reflectance and noise are minimized. These images were then processed with PCA to yield score images of the defaced test samples. The score image resulting from the image containing the most information of the original image, PC1, rarely contained any hint of the defaced serial number, but the score image of higher numbered principal components, like PC7 or PC10, appeared to contain a significant amount of this information. Usually one of the principal component score images looked very much like a number, while the others did not, although in many cases there appeared to be hints of that number present in some of the other higher numbered principal components. The coupling of the LIT method with the PCA treatment appeared to give good results in many cases and use of the chopped laser as the heating source appeared to give the best results. Using this combined method, several of the experimental parameters were systematically altered in the LIT experiment to determine the best conditions for serial number recovery. These comparisons were largely based on a visual analysis of how closely the best looking score image resembled the original serial number before it was defaced. Some parameters were varied in an attempt to find the best recovery parameters including preparation of the surface including polishing and coating the surface to maximize absorption of the laser pulse, the intensity of the laser, the initial temperature of the sample, and the pulse rate of the heating source. Good results were obtained for several different combinations using a defaced number 2 on the steel "graded sample"

Attempts to take the human part out of the comparison of score images to the number library were made through implementing similarity merit measurements. In order to use the similarity measurement, the score images had to be further processed using the Zernike Moment Analysis (ZMA). This provided an image vector that was the same size for any score image or number library image. The PCA-ZMA analysis combination then was used to calculate several similarity merit measures which were a mathematical comparison of the similarity of a particular score image or the whole set of score images to a set of library images.

Several "similarity merit" measures are available for this purpose and are available for MATLAB. The following methods were some of those used in these studies to measure the similarities between recovered serial numbers and library sets of pristine undefaced numbers between 0 and 9: cosine θ , Euclidean Distance, Determinant, Unconstrained Procrustes Analysis, Constrained Procrustes, Mahalanobis Distance, Pooled Mahalanobis Distance, Bartlett Stats and Correlation coefficient. These similarity measures utilize different characteristics of vectors to make comparisons between them, eventually resulting in a similarity value that defines how similar or dissimilar the vectors are within the characteristic captured by the measure.

Employing several of these measures to compare the score images to the library ensures that different defining characteristics including angle between the vectors, the distance between vectors and the transformation necessary to make one vector similar to another, are captured and used to give a holistic comparison between the recovered numbers and the library. The similarity measures were combined together using a set of fusion rules. The fusion of these similarity measures was then used to select the best match either through the minimal value of the sum of the normalized values of the similarity measure, and/or using a majority vote method where the number is identified as one with a majority of low values. The mathematical equations associated with these similarity measures are given in Appendix 1.

The PCA-ZMA analysis combination with the similarity merit evaluation was applied to the “**graded sample**”, the defaced numbers 6, 2, 5, and 0 in a steel sample that was defaced by a machinist to continuously increasing depths. The highest merit values assigned between the 6 in the defaced sample and the 6 in the library, and likewise for the 2 and the 5 were achieved using all 15 score images matched to the library using the PCA-ZMA analysis. .

The LIT method with PCA-ZMA processing and similarity merit measurements was also applied to a real world sample, a 12 gauge shotgun barrel with the text "*12 Gauge*" stamped into the barrel. The numbers *1* and *2* were defaced and re-polished using sandpaper of two grits. The barrel was placed into the LIT experimental setup and phase images were computed and then analyzed with the PCA-ZMA method followed by comparison with numbers in a library using the similarity merit measurements. The results from this showed that the defaced number 2 was identified as the number 2 in the library using all the score images based on this comparison having the highest sum of merit values from 10 different similarity merits. The italics number *1* had the second highest sum of merit values, with a number 4 having the highest. However the number library used for the comparison did not have an italics number 1 in it. Another defaced serial numbers set was recovered from a set of forceps with a laser engraved serial number using the LIT with PCA-ZMA processing. In all studies, the approximate position of the defaced number was known. Two papers were published in the *Journal of Spectral Imaging* in 2019.^{1,2}

It should be noted that some unexpected difficulties were encountered in performing these studies. The laser system that was used for our previous grant stopped working and had to be replaced. This cause a significant delay in starting our studies. Once the studies began, the pulsing circuitry used to synchronize the heat pulse of the laser with the acquisition of the frame rate of the camera collecting thermal images during the heat pulse degraded. There was a noticeable drift in the timing. It was replaced by a commercial system an FY 6900 Dual-channel Arbitrary Waveform Signal Generator. Additionally, due to constraints imposed by travel restrictions starting in March 2020, we were limited to collaboration with the Idaho State Police Lab, and the Utah Lab did not participate in these studies.

II. Work Performed

The work performed is divided into five sections consistent with the overall aims defined in the project description as presented in the Introduction. Since the bulk of this work was performed with similar lock-in thermography (LIT) instrumentation and the image analysis using

the principal component and Zernicke or pseudo-Zernicke moment comparison described in the final report of the related grant "Infrared Thermal Imaging for Use in Restoration of Defaced Serial Numbers" # 2013-R2-CX-K012 and in the two manuscripts published in the *Journal of Spectral Imaging*.^{1,2}, no in-depth description of these will be provided. Information will be provided if significant changes exist in the instrumentation, procedures, and/or analysis methodologies.

IIA. Surface Prep and Recovery Depth

Preparation of the defaced metal surfaces, in terms of the amount of both polishing and painting of the surface, was expected to reduce effects of emissivity differences, and determination of the correct polishing and painting techniques proved to be an essential part of the project. Studies were performed to examine the effect the surface preparation on the quality of the serial number recovery. In the previous grant, a single coat of black barbeque paint or India Ink was applied to the surface of the metal sample in the defaced area after it had been polished using the "doctor blade" method. In the doctor blade method, a single layer of cellophane tape is applied to the metal surface to make a well in the defaced area. Next several drops of paint are added at the edge of the well and a microscope slide is dragged across the surface. This provides a single coat of black paint over the defaced area on the metal. The purpose of this is to black painted area is to make the surface above the defaced number, an area that will absorb the pulsed laser light and reduce the emissivity of the surface. The first of the studies performed here was to determine the optimum number of coats of black paint required to optimize the serial number recovery. In the first two figures below, a visible image of the "graded sample" made of stainless steel with its original number, as-stamped, is provided along with the visible image of the same sample after being defaced by a machinist with each successive number defaced further by taking off more of the metal surface.



Figure 1. Original graded sample, as received from the company.

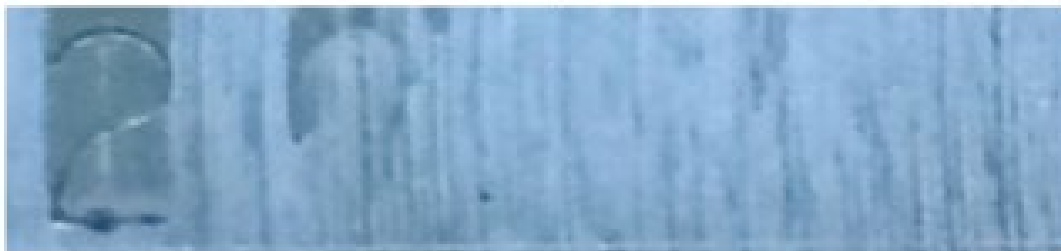


Figure 2. Graded Sample after being defaced.

In one case shown here, using a 2 W green-colored laser as a heating source, lock-in thermography coupled with multivariate image analysis, was applied toward the recovery of the defaced number 6, the second 2, and the defaced number 5. In the first figure, the defaced sample was painted with only one coat of black paint, and in second figure below it the defaced sample was painted with two coats of black paint.

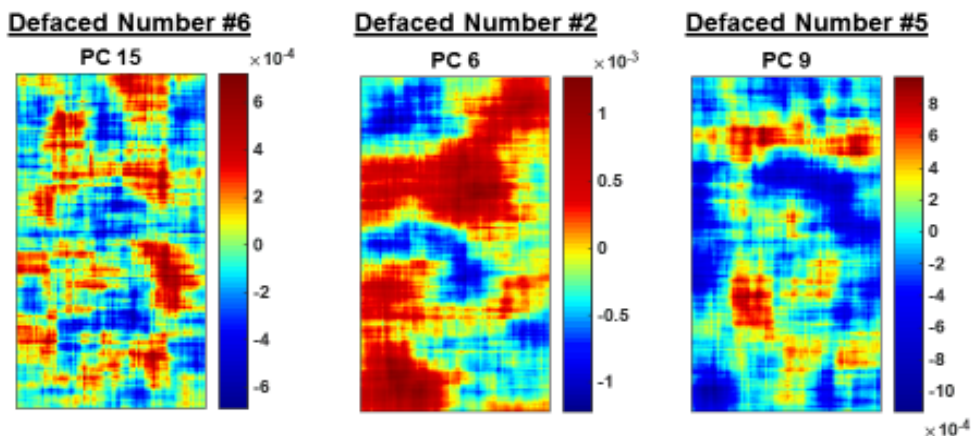


Figure 3. PCA image most representative of the original number for samples prepared with one coating of black paint.

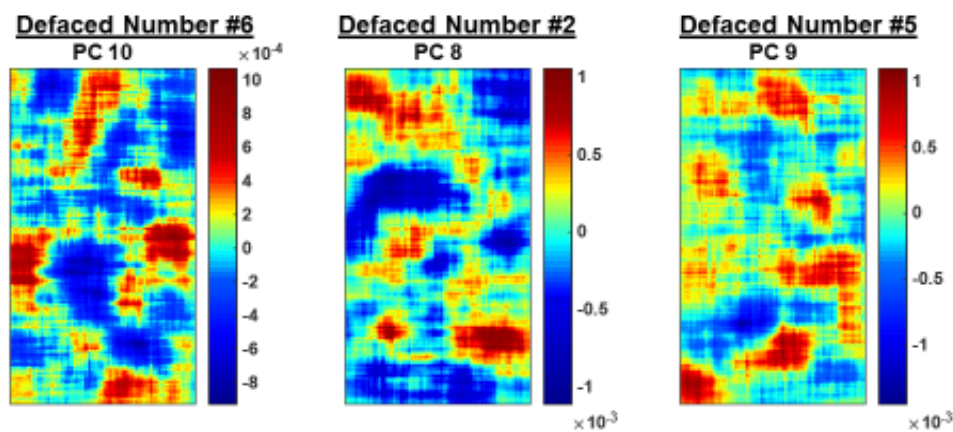


Figure 4. PCA image most representative of the original number for samples prepared with two coatings of black paint.

Based upon this set and other sets of studies performed with the defaced samples painted with 1, 2, and 4 layers of paint, a single coat of paint is best, although two coats will also allow recovery of the defaced number. Attempts to recover the defaced numbers coated with 4 layers of paint were largely unsuccessful. It appears that the extra layers of paint may not integrate well with each other since subsequent layers are applied after the other ones dry. This may prevent substantial thermal transfer from the black paint layers to the metal surface and bulk structure of the defaced material.

With regard to polishing of the sample, as expected, polishing with only sand paper of grit 400 or 600 left ridges in the metal defaced sample area. Thermal images of the high and low parts of the ridges conveyed different temperatures in the thermal images, assumedly the high parts emitted a higher temperature than the low part. This affected both the raw thermal images and the processed amplitude and phase image. Generally speaking, there was more evidence of the ridges in the amplitude images. Further polishing using 1000 or 1200 grit sandpaper reduced these thermal fluctuations.

The graduate student on the project, Anit Gurung suggested that simply applying a layer of black electrical tape might perform the same purpose as the black paint, and that if used, then the surface of the metal should be at room temperature, rather than at $\sim 70^{\circ}\text{C}$ as was done in the previous studies using the black paint. To test this, black vinyl electrical tape was placed on the surface to cover both the undefaced number 2 and the partially defaced number six from the **graded sample**. Figure 5 shows the improvement in thermal emissivity difference for precise measurement of apparent surface temperature.

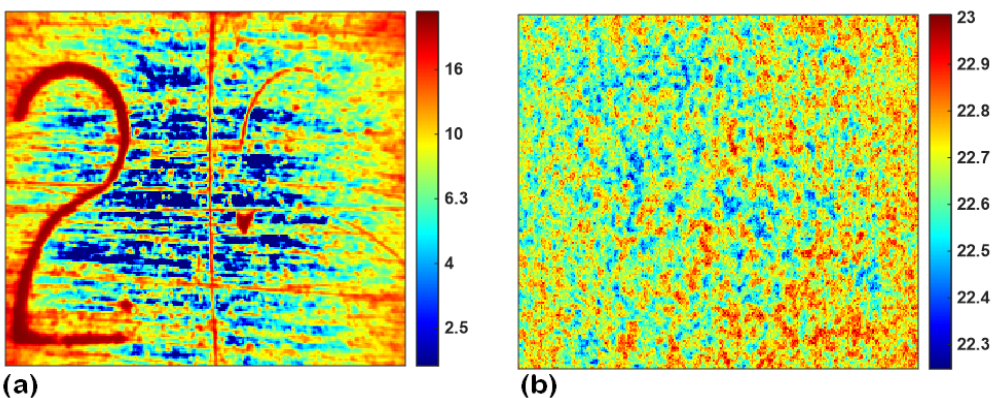


Figure 5. Thermal imaging with no external heating of serial numbers, 2 (non-defaced) and 6 (partially defaced), on a stainless steel: a) without a black electric tape and b) black electric tape on the surface

The numbers are not visible in the thermal image of the defaced area with the black electrical tape. This area now shows the same surface features even with its different subsurface features. This uniform emissivity as shown in the thermal image proved helpful in determining the lock-in frequencies that would provide phase images of the defaced serial numbers.

Use of the calculated phase image from the lock-in thermography signal can reduce the signal due to noise associated with the environment. However, choice of the lock-in frequencies that will best reveal subsurface defects is difficult if there are large emissivity difference. Use of the black electrical tape as a uniform cover for the defaced surface, allowed for determination of the best lock-in frequencies through the following method. After applying the tape, the test sample was then placed underneath the IR camera at room temperature. The non-sinusoidal (square) thermal excitation (heating and cooling for each half of the lock-in period) was

performed by targeting laser pulse to the surface. The temporal thermal images (frames) were collected at an equal time interval with varying lock-in frequencies to analyze the optimal lock-in frequency for feature extraction. A fixed number of frames (thermal images) per lock-in cycle, here 8 frames per cycle, were recorded for uniformity. Four thermal images were recorded when the laser is on and the other four images when the laser is off at each period. The variation of lock-in frequencies and the frame rate for each lock-in period is presented in Table 3-3.

Table 1. Tabulation of Lock-in frequencies and the respective frame rate

Lock-In Frequency (Hz)	Frame Rate (Hz)
0.0125	1
0.25	2
0.5	4
1	8
2	16
4	32
8	64

Lock-in thermal images for undefaced 2 and partially defaced 6 were collected and the phase (ϕ) and amplitude (A) images were computed at all the lock-in frequencies mentioned in Table 1. Figures 6 and 7 show the features of thermal, phase, and amplitude images at different lock-in frequencies for the undefaced two and partially defaced six, respectively.

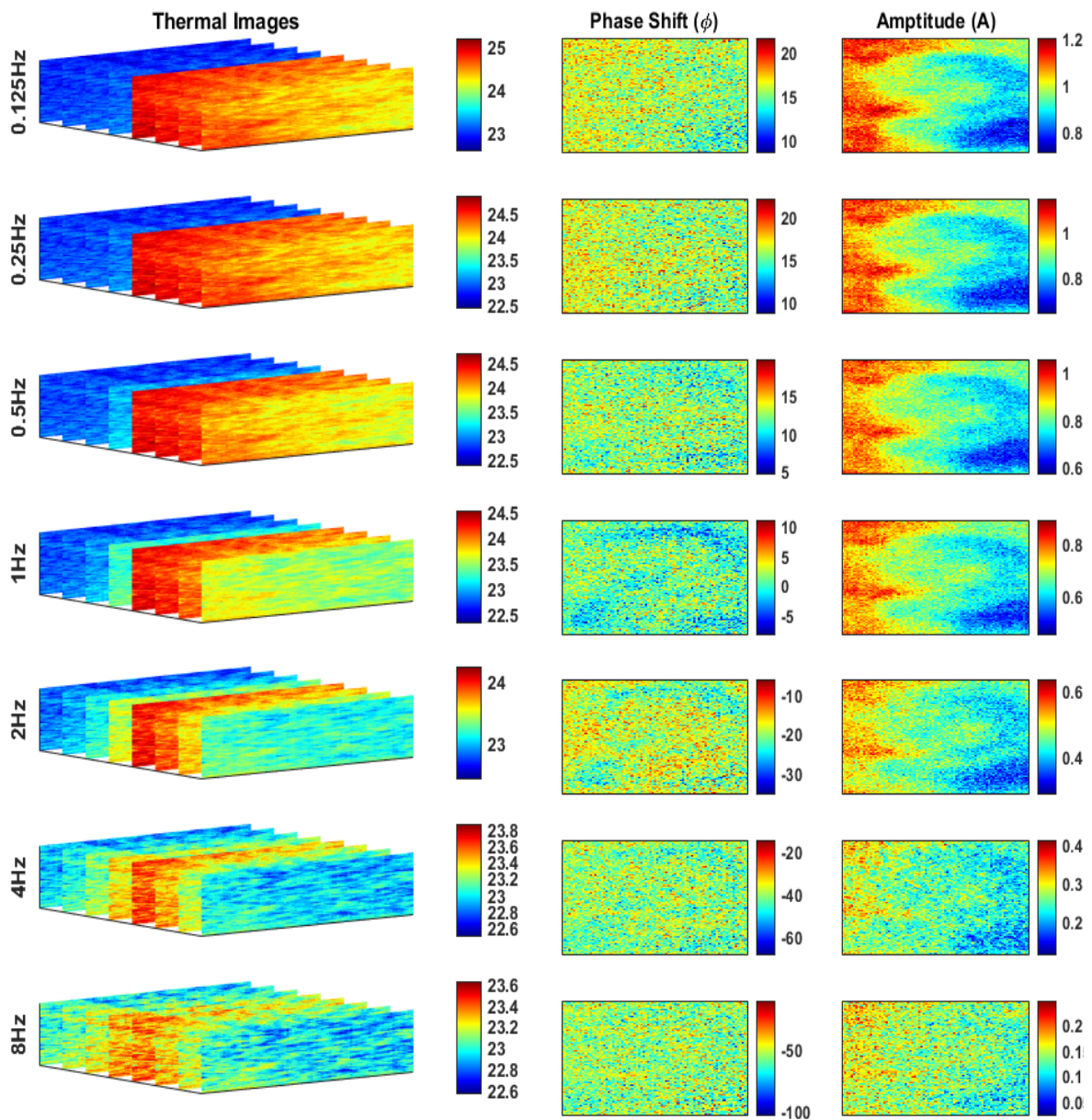


Figure 6. Thermal, Phase (ϕ), and Amplitude (A) images for undefaced 2 at each 7 different lock-in frequencies (0.125, 0.25, 0.5, 1, 2, 4 and 8Hz)

As the lock-in frequency increased, the change in temperature decreased. At 8Hz, the temperature change is approximately 1°C, whereas the lock-in frequency of 0.125 has a variation of about 2.5°C. The amplitude image extracts features from the surface or [very near the surface](#) and is hugely affected by the occurrence of a temperature gradient observed in the thermal images. The temperature gradient is caused mainly by the uneven distribution of laser power across the sample surface, some variation in surface emissivity, and IR camera's field of view. However, the temperature gradient does not hurt the phase images as the feature extracted is

underneath the surface. The lock-in frequency defines the depth of subsurface that is being analyzed. The phase image at 1Hz seems to have extracted the features of number 2, which can be observed visually. Frequency of 0.5 and 2Hz also have some features, but not entirely clear, as seen in 1Hz. The lock-in frequency analysis for undefaced 2 indicated that the optimal rate was close to 1 Hz, which could vary from 0.5 to 2 Hz. For more verification, a similar analysis to optimize the range of lock-in frequency was done on the partially defaced 6, shown in Figure 7.

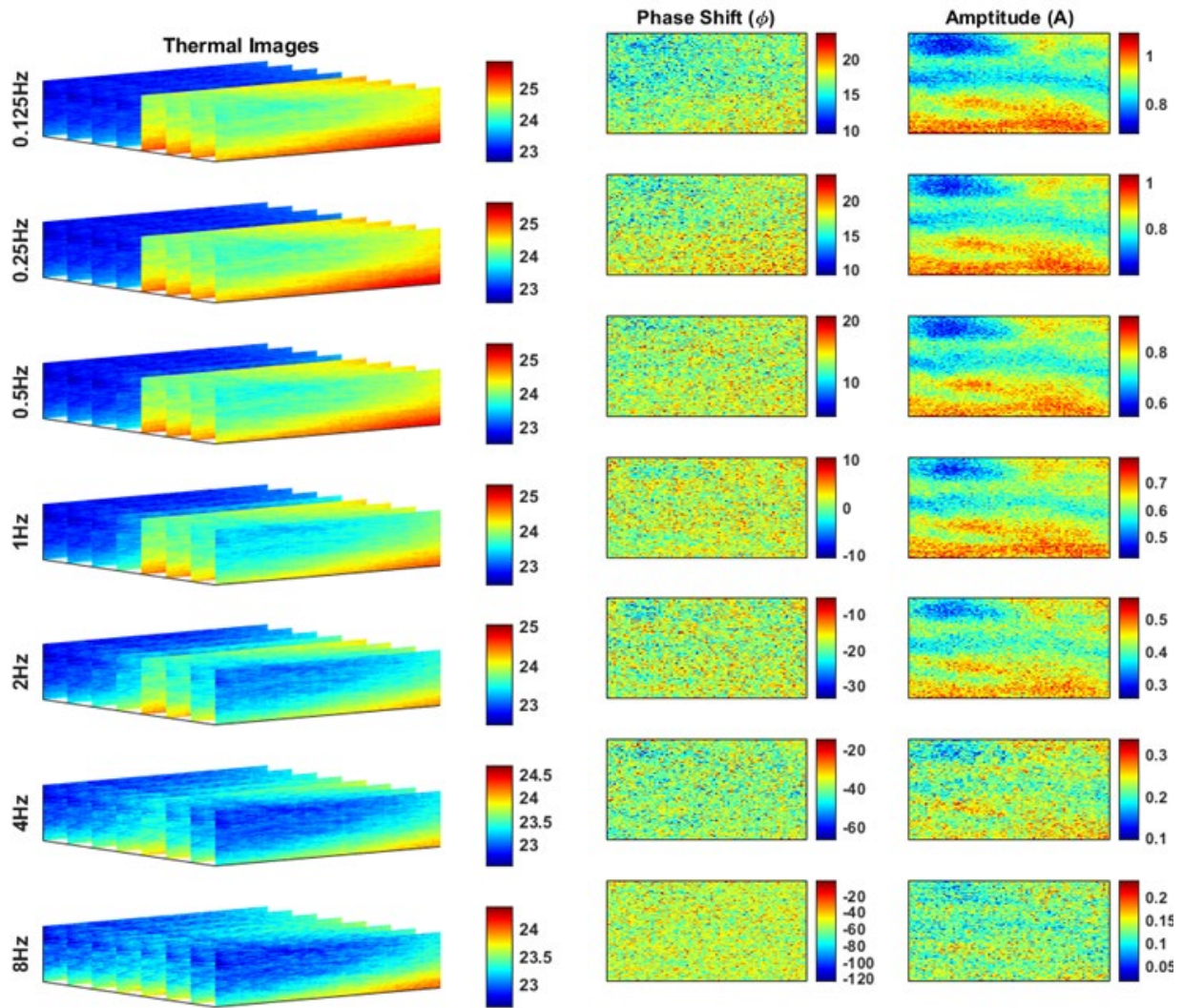


Figure 7. Thermal, Phase (ϕ) and Amplitude (A) images for partially defaced six at each 7 different lock-in frequencies (0.125, 0.25, 0.5, 1, 2, 4 and 8Hz)

In this experiment, the amplitude was also slightly affected by the temperature gradient as a similar trend between amplitude and thermal images is observed in Figure 7. The phase image seems to be the choice based on previous analysis. Note that in this case, the resolution of the phase image is not high enough for unbiased visual identification of the partially defaced number 6. The pattern cannot be clearly defined by either lower or higher phase shift values and further

image processing is needed for identification. These results suggest that determining the range of optimal lock-in frequencies may have to be based on a visual review of phase images associated with an undefaced number, such as the undefaced 2.

An additional result of these studies with the black tape was that if an adequate lock-in frequency can be identified, for the defaced sample, then the phase image is relatively free of environmental contributions, and a modest laser power of 1.5 Watts provides for a larger temperature swing than it does when the sample is preheated to 70°C as it was in our previous work. with a defaced metal sample at room temperature. Based on the thermal images presented in Figures 6 and 7, the temperature swing over the laser pulse was as large as 2°C at a lock-in frequency of 1 Hz, and decreased to slightly less than 1 °C at 8 Hz.

The above analysis to find the correct lock-in frequency is a reminder that there should be a defaced depth limit, beyond which the serial number cannot be recovered. To investigate this aluminum, steel, and rolled steel stamped samples were obtained from Precision Forensic Testing and given to a machinist to deface the serial numbers by preparation of series of steps, machined to increasing depths below the point where the number is completely removed. Thus for instance in the Aluminum sample described below, the depth of Step 1, 0.009”, is the machined depth where the first number of the serial numbers is just barely still visible. Step 2 is machined further down by another 0.012” to a total depth of 0.021”; Step 3 is machined further down by another 0.012” to a total depth of 0.033” and so on. It was necessary to deviate from the proposal due to limitations with the milling equipment. The width of each step of increasing depth would be widened to include two numbers rather than just one number. Since there are a fixed number of serial numbers stamped in the samples received from Precision Forensics Testing, this meant that the ultimate defacing depth was not as deep as indicated in the proposal. The defaced serial numbers and machined depths were:

Aluminum

5	Step 1	Depth 0.009”	0.23 mm
8	Step 2		
2	Step 2	Depth 0.021”	0.53 mm
9	Step 3		
1	Step 3	Depth 0.033”	0.84 mm
6	Step 4	Depth 0.045”	1.14 mm

Steel

1	Step 1	Depth 0.004”	0.10 mm
8	Step 2		
6	Step 2	Depth 0.016”	0.41 mm
3	Step 3		
4	Step 3	Depth 0.028”	0.71 mm
8	Step 4	Depth 0.040”	1.02 mm

Stainless Steel

9	Step 1	Depth. 0.013 “	0.33 mm
6	Step 2	.	
0	Step 2	Depth 0.025”	0.64 mm
1	Step 3		
5	Step 3	Depth 0.037”	0.94 mm
6	Step 4	Depth 0.049”	1.24 mm

The machinist also prepared the samples which were milled to increasing depths in a wedge-like fashion rather than in a stepped fashion.

The depth of defacing in Step 2 of these samples is comparable with the recoverable defaced numbers of the “**graded sample**” from our previous investigation. The defaced depths of Step 3 and Step 4 represent a larger depth of defacing than in the **graded sample**. Thus the defaced numbers on Steps 3 and 4 were meant to provide a measure of how deeply defaced the numbers could be and still be recoverable by the lock-in thermal imaging with image analysis and library matching, the LIT with PCA-ZMA processing developed in our previous grant.

In this first example, the 2nd step of the aluminum sample, the thermal imaging techniques were used on the area of the step where the digits 8 and 2 had been machined away. These sample here was machined to a total depth of 0.41 mm which was approximately 0.31 mm below the point where the number was no longer visible. Several different sampling parameters were attempted. The image below is the averaged phase image from 22 heating cycles, each cycle consisting of 32 frames taken evenly spaced over the 32 second long cycle with the laser power on the sample at 1.2 W. The results were somewhat mixed.

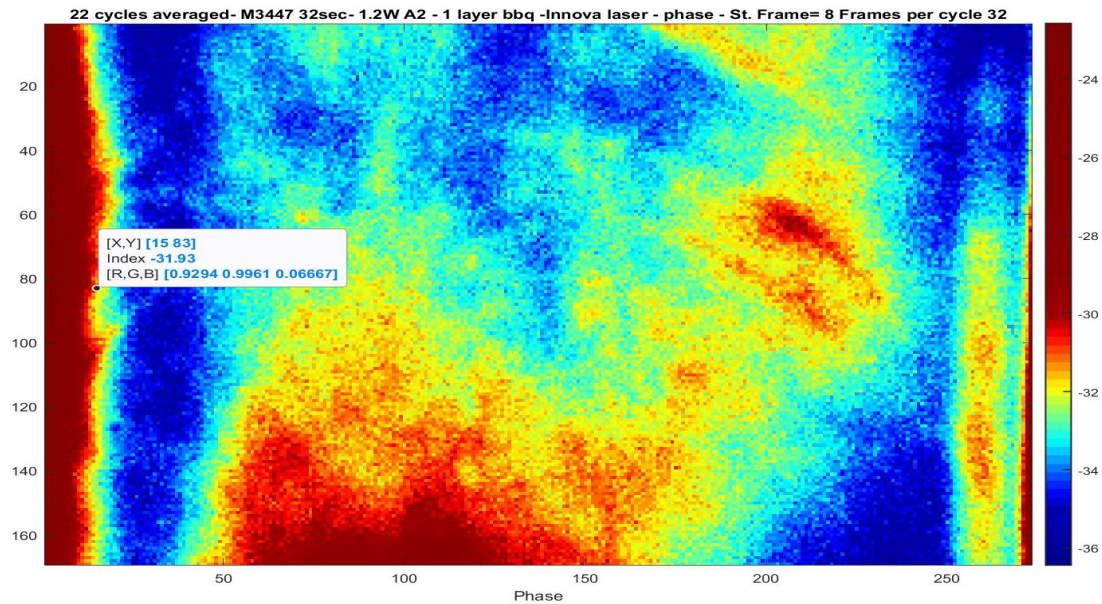


Figure 8. Phase image of the 22 cycle average from the 2nd machined step of the defaced aluminum stepped sample.

In roughly the area where the 8 was defaced processing of the phase images from the infrared camera gave the following score plots 2-12. It is not visually obvious that the pseudo-Zernicke (PZ) moments of these score plots should match best with an 8 from the libraries. The score plot that visually appears to match best with an 8 is score plot 12. The rotationally invariant matching program was modified so the user could select the score plot or score plots to be used in the matching algorithm.

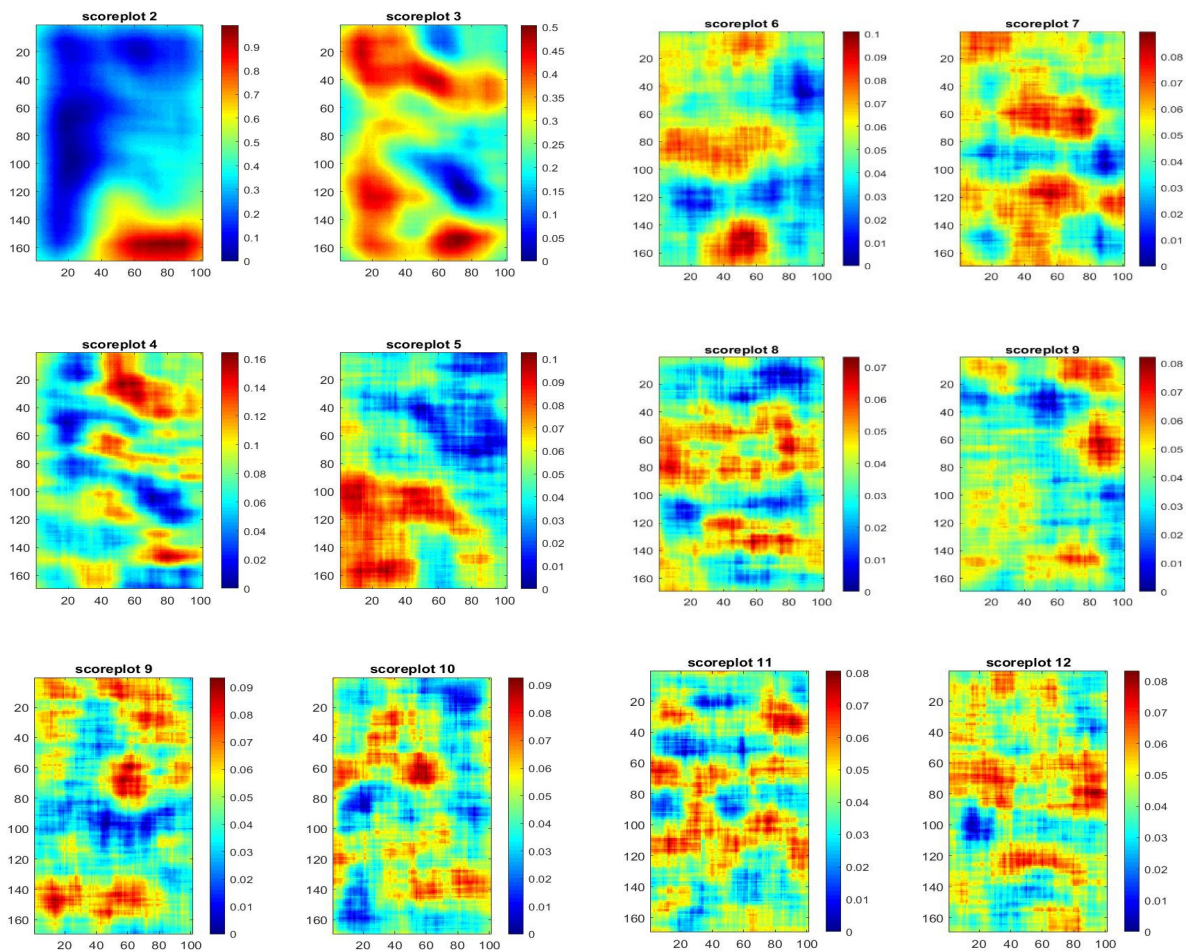


Figure 9. Score plots 2-12 in the region where the defaced 8 should be located.

Taking these images and performing a library match gave the following results.

Table 2. Results from the Majority Vote library matching for defaced 8 on 2nd Step.

Defaced Number	score plots used	Match Rank	Possible Numbers									
			0	1	2	3	4	5	6	7	8	9
8	s3-16	Match Rank	8	2	1	5	9	3	7	0	6	10
8	s6-13	Match Rank	0	2	1	0	9	4	8	5	6	10
8	s12	Match Rank	2	8	1	7	10	0	5	9	0	6

Note that when score plots 3 through 16 or just 6 through 13 were converted to PZ moments and used for the process of determining the best match to the values, the best match based on these score images was for the defaced number to be a 2, and the 2nd best match was for the defaced number to be a 1. The number 8 was ranked as the 6th best match in both cases. Also, if just a single score image, score image 12, the one that perhaps visually looked most like the number 8, was used in matching with the library, then the best match was still a number 2 followed, with the 2nd best match being a 0. The 8 was not even recognized as a viable match as evidenced by the 0 in the column under possible number 8. Note this was just for the case of one "movie" collected as described above. Several movies were taken, but analysis of several of the movies taken did not suggest that the 8 was a good match to the defaced number on the step in that area where the defaced 8 was indeed present.

Subsequently, infrared images were taken of the same defaced step, in the area where there should be a defaced 2 present. The score images corresponding to one of the several movies taken of this area of step 2 are provided here.

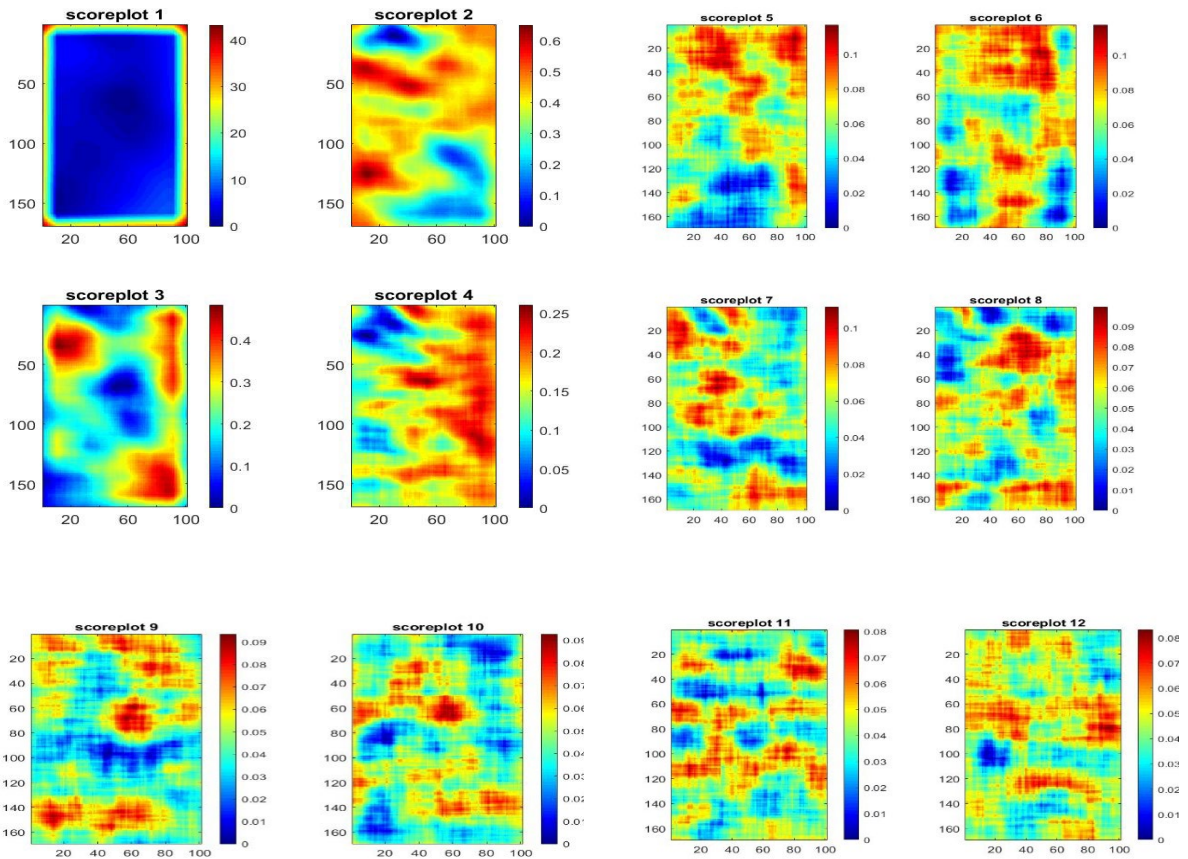


Figure 10. Score plots of the aluminum step sample from the area where the defaced 2 on the 2nd step should be present in the image

Here again, based on visual inspection of the score plots as compared to the numerical part of the library, it would visually be difficult to say that the best match for the defaced number is with a 2. Score 9 looks most like the number 2, and one might expect a good match between the score 9 image and the 2 in the library. The PZ moments of the score images were calculated and

compared with the PZ moments of the library numbers (only the numbers in the library for these studies). Two different match selections were tried, one based on score images 5-22 and the other based only on score image 9.

Table 3. Results from the Majority Vote library matching for defaced 2 on 2nd Step.

Defaced Number	score plots used	Match Rank	Possible Numbers									
			0	1	2	3	4	5	6	7	8	9
2	s9	Match Rank	4	6	1	3	0	2	10	0	0	0
2	s5-s22	Match Rank	6	3	1	4	9	2	8	7	5	10

Note that in this case, the best match of the score images of the defaced 2 was with the number 2 from the library. The second best match was with the number 5. So, from the attempts to recover the defaced numbers from the aluminum stepped sample, provided a 50% accuracy using the experimental parameters described above.

Similar experiments were performed on the steel stepped sample using a laser power of 1.5 W at the sample, 22 cycles, and 32 video frames per cycle. The image below is the averaged phase image from the stainless steel sample.

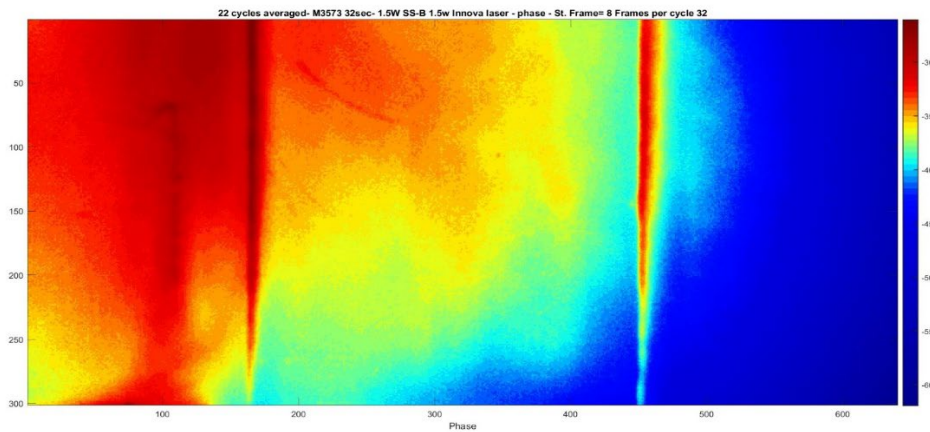


Figure 11 . Phase image of the 22 cycle average from the 2nd machined step of the defaced steel stepped sample.

As in the case of the aluminum sample, a defaced number 8 was present on the defaced step that was analyzed. There was also a defaced 6 present on that step. The score image from the area with the defaced 8, which perhaps visually looked like it would have the best match with the 8s in the library was score plot 10 from the amplitude image. The black and white (BW) image from this score plot is shown below. Also shown below is the BW image from the amplitude image of score plot 9 which was taken in the area where the defaced 6 should be present. This image looked most like the library images of a 6.

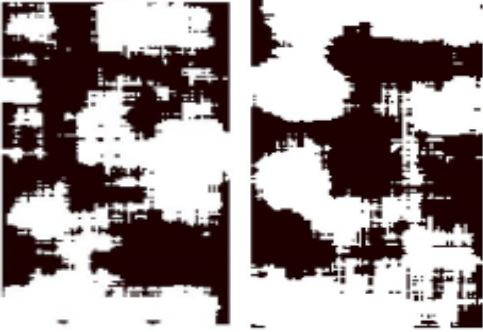


Figure 12. Left - Black and white image from the amplitude image in score plot 10 visually the best match for the defaced 8. Right – Black and white image from the amplitude image of score plot 9 in the area of the defaced 6.

Taking a selection of the score images, finding their PZ moments and then using similarity merit measures and fusion rules to compare the PZ moments of the score images with those in the library gave the following results.

Table 4. Results from the Majority Vote library matching for the defaced 8 and defaced 6 on the stepped stainless steel sample.

Defaced Number	score plots used	Match Rank	Possible Numbers									
			0	1	2	3	4	5	6	7	8	9
8	s5-s15	Match Rank	3	4	2	0	10	1	6	0	0	8
8	s10-s13	Match Rank	3	9	1	0	10	2	8	4	0	7
6	s5-s15	Match Rank	7	5	1	0	10	2	8	0	0	9
6	s9-s10	Match Rank	0	7	2	0	10	1	0	9	3	8

Note that in this case for both the defaced 8 and defaced 6 on the 2nd Step, the library match with the PZ moments of the score images was inadequate for identification of the defaced numbers. In the case of the defaced 8, use of a large number of score images for the PZ moments gave the resulted in inability to match with any of the library numbers as evidenced by the 0 in the column under possible number 8. The identification of the defaced 6 faired only slightly better. When only the score images that “visually” looked most like a 6, score 9 and score 10, were used, the number six, was the 3rd top choice behind a number 5 and the number 2.

A similar analysis of the defaced numbers stainless steel samples with the defaced numbers was also initiated. The image below is the averaged amplitude image from 22 cycles, each cycle consisting of 8 frames taken evenly spaced over the 32 second long cycle with the laser power on the sample at 1.5 W.

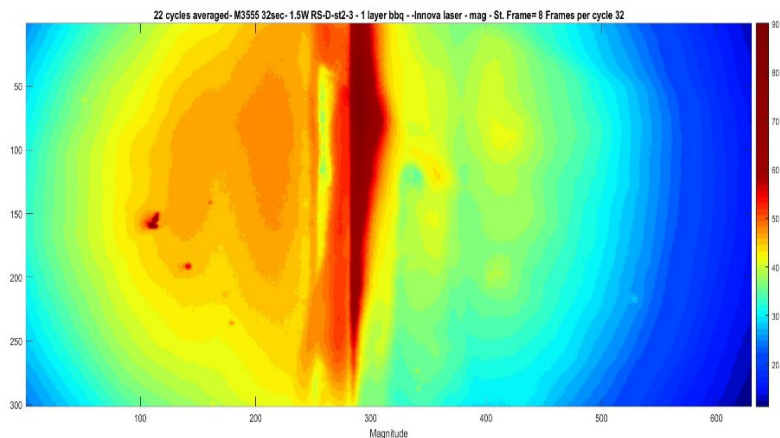


Figure 13. Amplitude image of steps 2 and 3 from the stainless steel sample.

As before, principal component analysis of the amplitude images from the 22 cycles resulted in 22 score images. A subsequent comparison of the PZ moments of the score images with the PZ moments of the library yielded disappointing results, similar to those obtained for the steel sample.

Based on the difficulty encountered in adequately recovering the defaced serial number from Step 2, and the likelihood of even less success at recovering numbers that are defaced to deeper depths, the studies were concluded. From these results, it is likely that the maximum depth recoverable with laser heating from about a 2 W laser is in the range 0.5 mm or 0.02”.

Because there were problems recovering the defaced numbers from the stepped samples made by the machinist, other defaced samples were acquired as well to help determine if the inconsistencies in recovering the numbers were due to the machining of the samples, from the experimental procedures, or a limitation in the ability of the technique to recover the serial numbers. Collaborative Testing Services (CTS) Forensics produces a test sample for serial number recovery, twice a year, that are used by many forensics labs across the country to test their abilities at serial number recovery. They provided test samples from previous years, one of which was analyzed with the thermal imaging technique.

The CTS Forensics previous year test sample used in the thermal imaging study was made of zinc. For this test sample, there is no information given about the absolute positions of the numbers; one only knows the larger area where they have been defaced on the metal sample. They provide information on some possibilities for the defaced characters and on the font and height and width of the numbers. In this particular test the possible characters were:

0,1,2,3,4,5,6,7,8,9,A,B,C,D,E,F,H,J,K,M and N

The samples were first sanded to remove the toolmarks from the mill tool used to deface the serial number, and the surface was painted with 1 layer of black paint using the doctor blade technique.

The results obtained from testing on the sample made of zinc are given here. For these unknowns, the correct orientation of the sample must be determined. Figure 14 shows the size of the defaced area relative to the characters. There were 6 characters stamped into this space. The exact vertical and horizontal position of the characters were unknown although the CTS unknown sample had an aluminum bar included with the unknown. This aluminum bar had all the serial stamp characters and the relative spacing of the characters with respect to one another provided on this aluminum bar included with the zinc unknown. Figure 14 is a picture of the defaced zinc sample after it had been polished with very fine sandpaper, and painted with black paint.



Figure 14. Picture of defaced CTS zinc test sample after sanding and applying black paint.

As mentioned above, the defaced space is large, and the correct sample orientation to view the characters must be determined by trial and error. The numbers that have been defaced on the zinc bar can be oriented horizontally or at 180° to the initial horizontal orientation. An initial orientation is chosen, and then once the first characters have been located, the orientation can be re-evaluated.



Figure 15. Photo of initial sample orientation chosen to view the characters. Blue rectangle shows approximate camera view of sample for this movie.

To find the first characters, camera frames are taken over several heating cycles as in a normal experiment. Cycle times and number of cycles are varied since the recovery may be best for a particular cycling time. These cycles are converted to phase images. A disturbance in the phase images derived is thought to be associated with the presence of a defaced serial number. For the zinc sample, there appears to be a defaced number disturbance as seen in Figure 16.

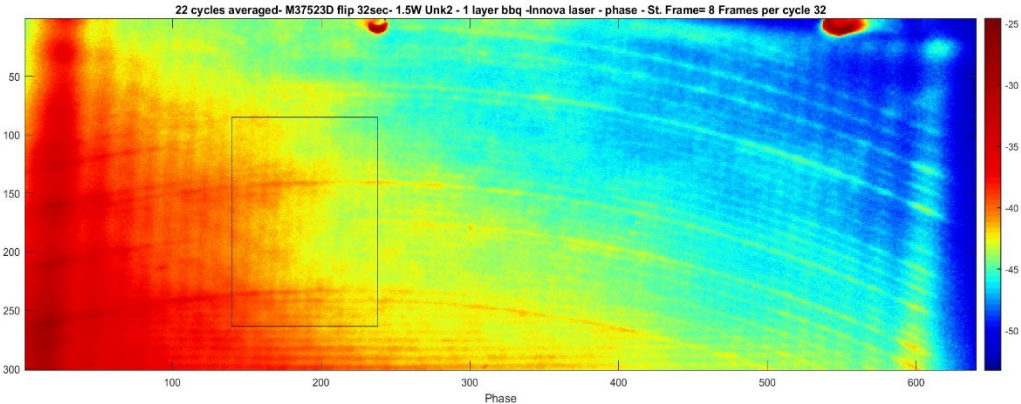


Figure 16. Phase diagram of full width of camera view for 8 frames per cycle and 22 cycles averaged. Box shows possible disturbances in the pattern that could be a number “2”

Currently, the program is not sophisticated enough to perform this search on a larger scale and this must be done visually by collecting several “movies” of 22 cycles with 8 frame per cycle and examining each of the movies for a disturbance in a similar area. Also, as noted in the previous discussion on reproducibility, it appears that one particular score image may contain the image of the defaced character more reproducibly, so if one particular score image contains a character in several movies, then that character is likely the identity of the defaced number. The initial identification of the score image to use is currently a decision made by the person processing the movies and producing the score images. Alternatively, a larger set of score images could be used and the sum of the fusion from the library matching could be used and would be independent of using one particular score image. There still would be some decision making involved, however, in terms of the number of score images to use for the library matching. In both cases which set of cycles to use in making the score images is also a consideration that must be decided by the user. In the reproducibility studies above, using all of the cycles taken generally gave good results, but in some cases, at least for the defaced number “6”, using less than the full set gave better results than using the full set.

For the zinc sample, a combination of library matching and fusion sum of one score image and using library matching and the fusion sum from several score images, usually 15. Additionally, the student or technician would visually compare the score image with the characters in the fonts provided. This was done because the character library contained 10 or more fonts to have a variety of character shapes. As can be seen in figure 17 below for the area identified in figure 16 as having a disturbance, score plots 5, 6, 7, and 8 all seem to have a “2” or possibly part of a “2” in them.

Score plot 5

Score plot 6

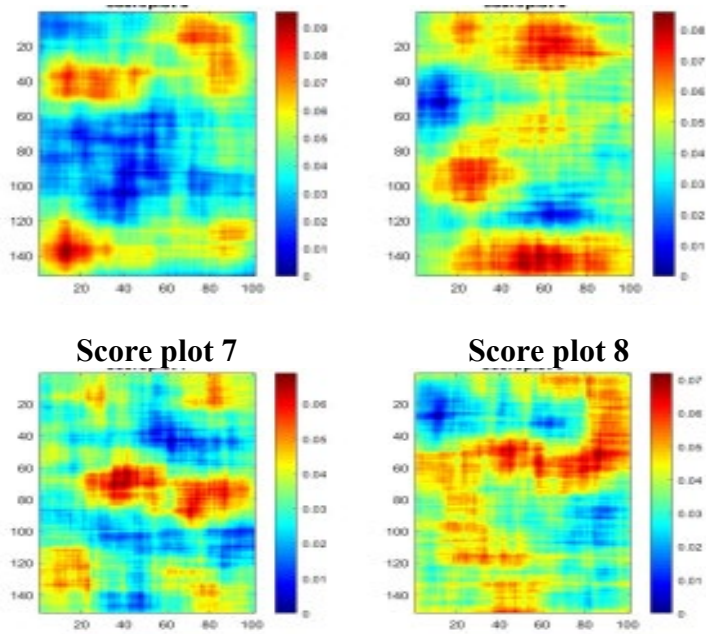


Figure 17. Score plots 5, 6, 7, and 8 derived from one movie of 8 frames per cycle and 22 cycles averaged. Score plot 6 looks very much like number 2.

Selecting just score plot 6 and looking at this same score plot for a few movies provided evidence that it was a “2”. If only score plot 5 was compared with the library, for one particular set of movies, the fusion sum gave the following values:

0 1 2 3 4 5 6 7 8 9 A B C D E F H J K N
 86 121 4 38 83 53 65 15 36 43 11 31 140 101 115 111 119 76 96 35
 whereas score plot 6 gave the following values:

0 1 2 3 4 5 6 7 8 9 A B C D E F H J K N
 115 116 88 77 56 6 27 137 74 101 45 60 39 104 15 43 130 144 8 60

Since the low value of the fusion sum is associated with the best fit, based on score plots 5 and score plots six, the defaced number would be a 2 or a 5. Visual inspection of the score plots suggests that the value is more likely a 2, and in other movies, score plots 5 and 6 suggest that 2 is the value of the defaced character. Now if the first 15 score images are all used to match with the library their fusion sum is shown in the following bar graph figure 27.

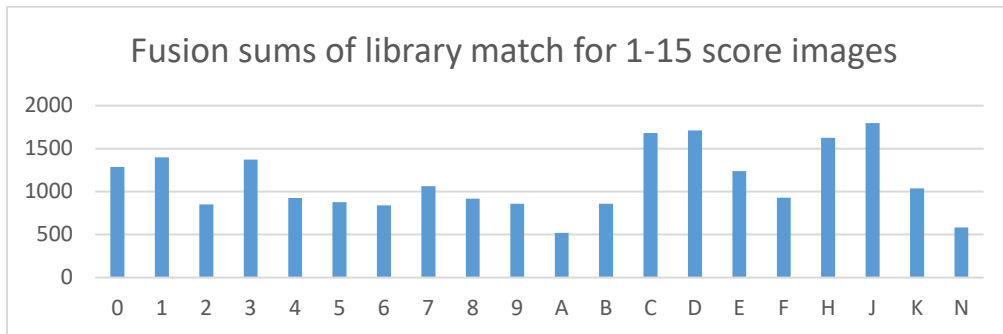


Figure 18. Fusion sums from library match to score images 1-15 for 4th character.

Note that here the lowest sum is for the character “A”, followed by an “N”. The “2” is in a tie for third place with the “6” and “B”. However, visually looking at the score plots in the middle region which are often more reproducible between several movies, identifying the character as a defaced “2” is reasonable.

Once the 2 was found and identified, then based on the number spacing provided with the examination materials, the placement of this “2” relative to the defaced area suggested that this was the 4th character from the left edge. There were a total of six defaced characters, and so using the position of the defaced 2 as an anchor, thermal imaging cycles were taken of the calculated position of the other characters. Similar numbers of frames, cycle times, and number of cycles were collected and the score images of the other defaced numbers were similarly derived and matched to the library.

These procedures of calculating the fusion sums for the individual score image matches with the library images, the fusion sums for all score images 1-15, and also a visual comparison, were carried out for all of the 6 character positions on the defaced zinc sample. The researcher performing this reported the following results:

Position 1 (closest to left edge)

B or possibly a 9 or D

Position 2

7 or possibly a 2 or a 5

Position 3

J or possibly a 9 or B

Position 4

2 or possibly a 5

Position 5

A or possibly a 4 or 7

Position 6

4 or possibly a 7 or 9

The true identity of the serial number was **D7J274**. The technician’s first pick for each defaced character was not always the correct character, but the correct character was present in the 2nd or 3rd possibility they identified for each character. Again, it should be noted that the identifying the position and possible identity of an anchor character is crucial to finding the rest of the characters. It is also worth noting that the stamp font was not directly used in the library during the comparison of the score images to the library and in fact several different fonts were present in the library. The results are somewhat promising in the sense that it appears the true character will be one of the top 3 picks, but there still is a high degree of human intervention especially with regard to the visual interpretation involved in finding an “**anchor character**” and in the visual comparisons performed in addition to the computer-based library matching based on the fusion sums.

Two important point learned from these studies were:

- 1) *The maximum depth of defacing, where the serial numbers may still be recovered using a ~ 2 W laser is approximately 0.5 mm below the surface of the stamped serial number.*
- 2) *The difficulty of recovering the serial number using the thermal imaging method increases greatly when the position of the number is largely unknown. Here a search for an anchor character must be done, and once that is found, the other characters are more easily identified.*

IIB. Score Image Contribution

From the results of our past study and in the information presented in the previous section, it was apparent that some of the score images were visually similar to the defaced number while others were not. In the past study, typically, all 15 score images derived from the PCA treatment of the phase images of the 15 heating cycles were used with the Zernicke or pseudo-Zernicke (PZ) moment analysis, and all 15 moments were compared with the moments from the library using the similarity merit measures. However, it would seem plausible that use of a subset of all of the score images, perhaps even just one score image, or even just the phase image itself might provide for a more robust and rapid recovery of the defaced numbers. Studies of whether using a particular subset of all the heating cycles to form the phase or score images, and then attempting to use that one score image to determine the identity of the number by matching with the library are presented in this section.

The first study was to see whether or not this would work for thermal images of an undefaced number, and if it gave reasonable results to extend it to a defaced number. The undefaced 2 from the **graded sample** was chosen as the focus of these initial studies. Studying an undefaced number provides a way to investigate the reproducibility of the imaging system and processing techniques, the effect of using different amounts of phase images to create a corresponding set of score images, and the viability of using of a single score image to compare the library and match with the number. These studies were performed on the **graded sample** by collecting lock-in thermal images over a total of 61 heating cycles. The following experimental conditions were used:

Laser power ~ 2.4 W at the sample Number painted with a layer of black BBQ paint
 Cycle time – 20 seconds 32 camera frames per cycle
 Sample equilibrium temperature on hot plate set at 70° C

A single, score image, PC4, which looked like a “2”, was processed and binarized according to the LIT-PCA procedures in the previous grant and its PZ moments were compared with those from the Library. One **important difference** is that in the previous grant, for almost all of the studies, the Library did not include the characters from the alphabet; it included only the number characters. Here the alphabetical characters are also included. In the next three figures below, score image PC4 was created from the first 15 cycles, then created from the first 20 cycles, and also created using the first 60 cycles. The PC4 score images are shown below in Figures 19-21 respectively. Also shown is are the results from comparing each of these PC4 score images with the library using the sum fusion of the similarity merits.

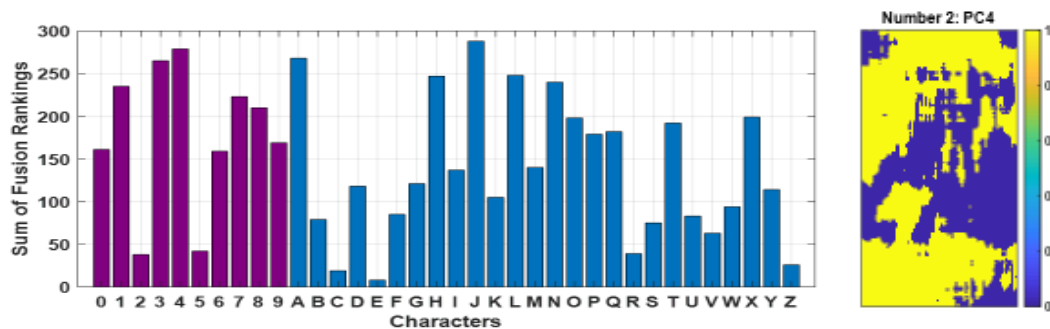


Figure 19. Score image PC4 derived from phase images of cycles 1-15 and corresponding character determination by fusion rules. (lowest sum of rankings is best fit)

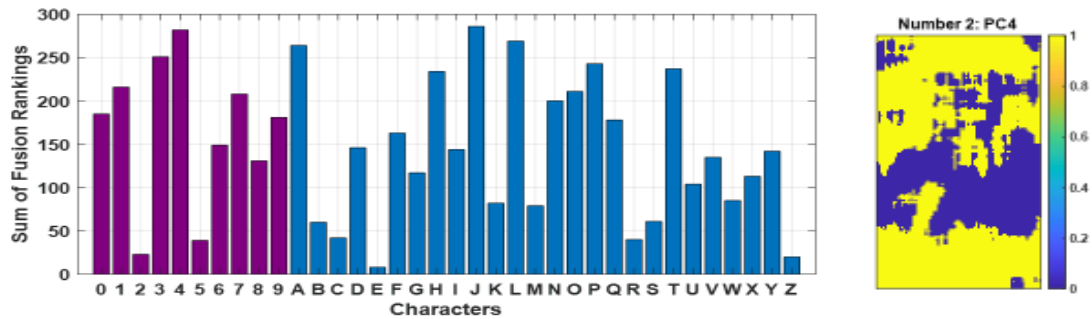


Figure 20. Score image PC4 derived from phase images of cycles 1-20 and corresponding character determination by fusion rules. (lowest sum of rankings is best fit)

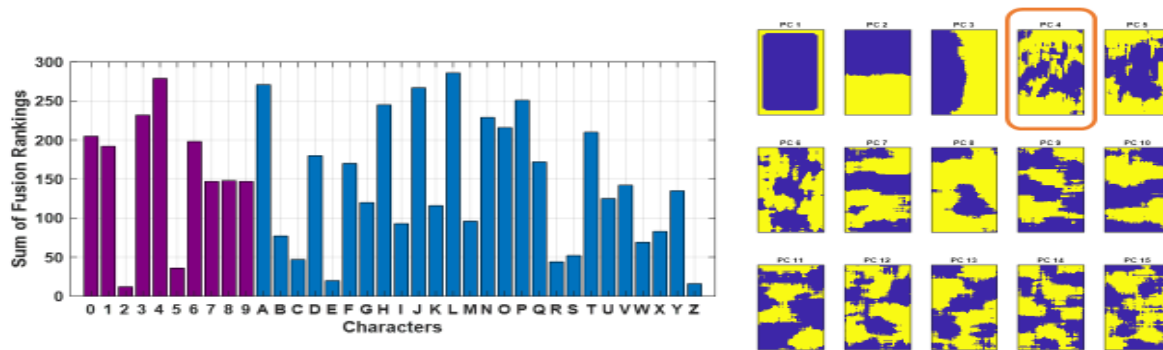


Figure 21. Score images PC1-15 derived from phase images of cycles 1-60 and corresponding character determination by fusion rules. (lowest sum of rankings is best fit)

Note that when only phase images from 15 or 20 cycles were used to compare PC4 to the library with the fusion rules, then number “2” did not have the lowest sum of the fusion rankings, but when 60 cycles were used to create the score images, then PC4 did show 2 was ranked lowest.

In the next set of experiment, also focusing on the undefaced 2 on the **graded sample**, the effect of leaving out some of the initial cycles was studied. Rather than always including the first cycle sets, different amounts of initial cycles were excluded. This was accomplished by collecting the following: phase images from all cycles except the first 5 cycles were used to create the score images; all cycles except the first 10 cycles; and continuing this process until only 10 score images were processed from cycles 51-60, and then 5 score images were processed from cycles 56-60. These are presented below in figures 22-32.

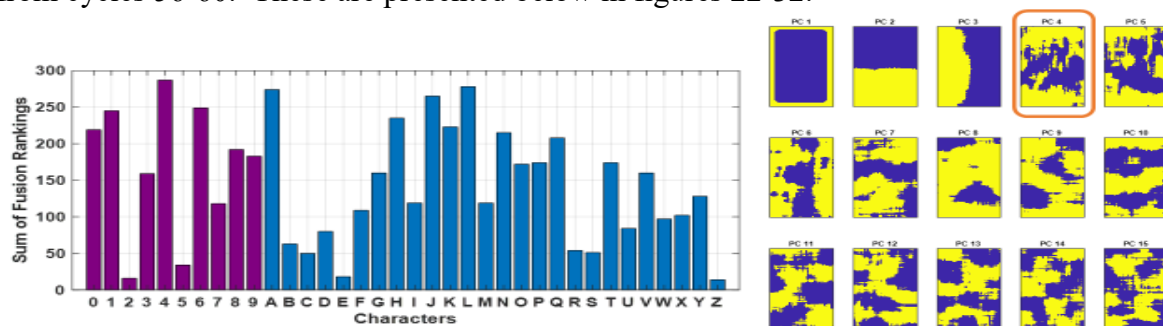


Figure 22. Score images PC1-15 derived from phase images of cycles 6-60 and corresponding character determination by fusion rules.

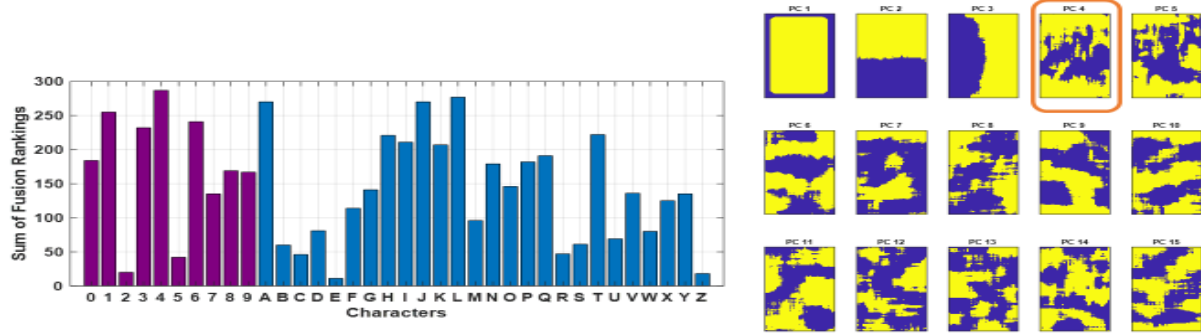


Figure 23. Score images PC1-15 derived from phase images of cycles 11-60 and corresponding character determination by fusion rules.

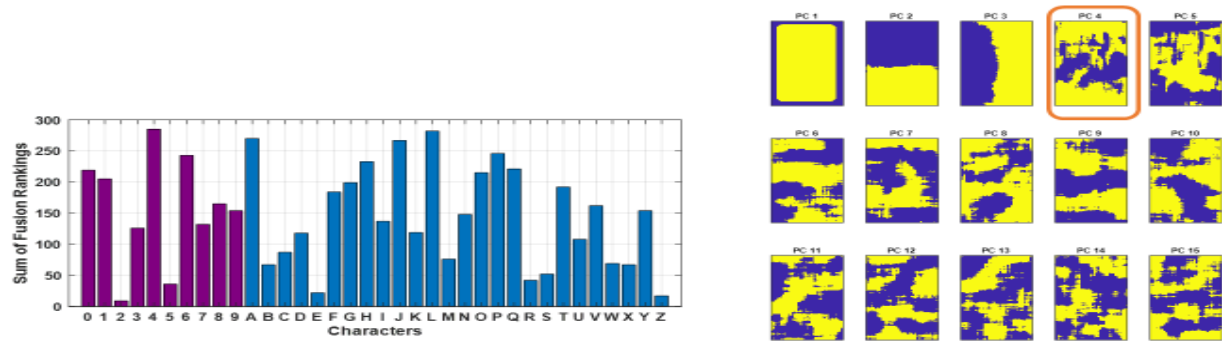


Figure 24. Score images PC1-15 derived from phase images of cycles 16-60 and corresponding character determination by fusion rules.

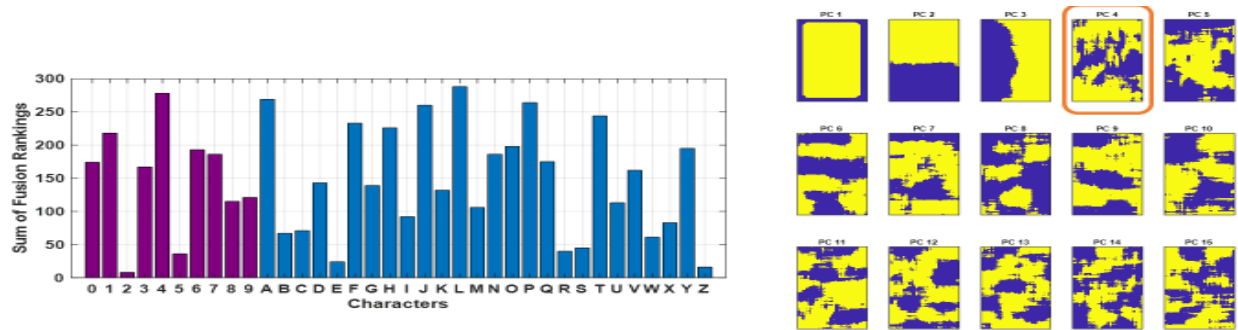


Figure 25. Score images PC1-15 derived from phase images of cycles 21-60 and corresponding character determination by fusion rules.

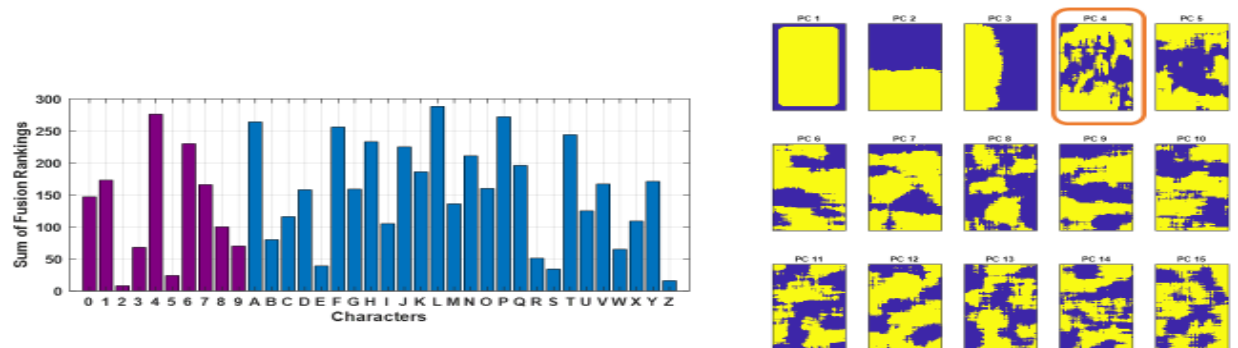


Figure 26. Score images PC1-15 derived from phase images of cycles 26-60 and corresponding character determination by fusion rules.

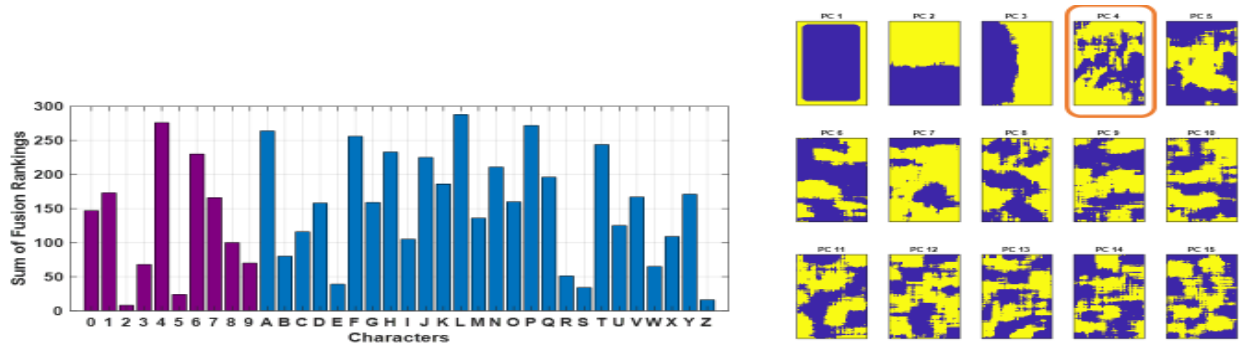


Figure 27. Score images PC1-15 derived from phase images of cycles 31-60 and corresponding character determination by fusion rules.

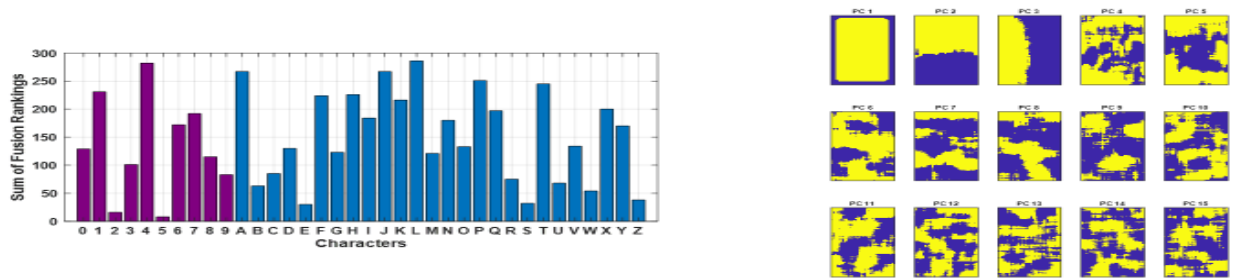


Figure 28. Score images PC1-15 derived from phase images of cycles 36-60 and corresponding character determination by fusion rules.

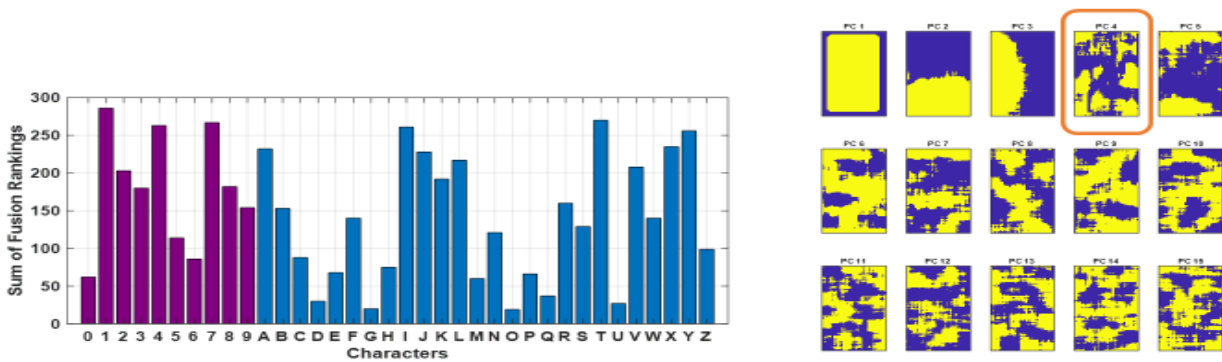


Figure 29. Score images PC1-15 derived from phase images of cycles 41-60 and corresponding character determination by fusion rules.

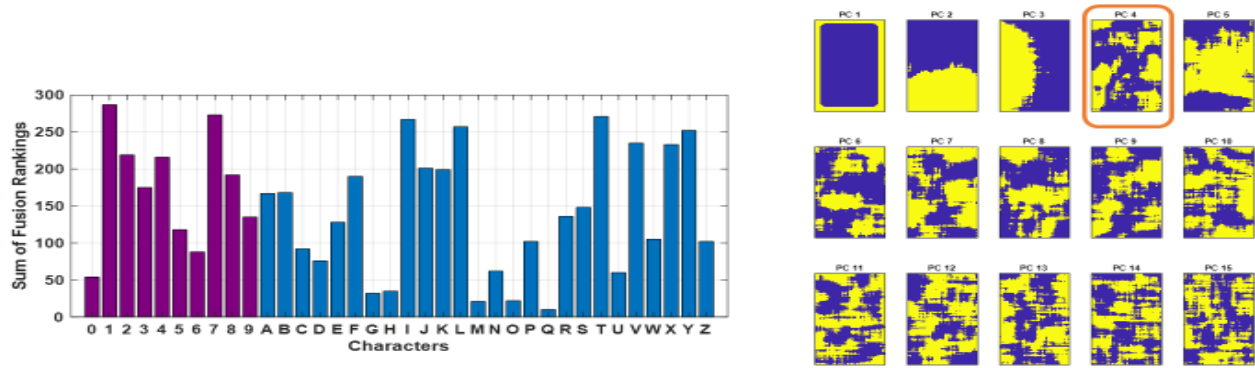


Figure 30. Score images PC1-15 derived from phase images of cycles 46-60 and corresponding character determination by fusion rules.

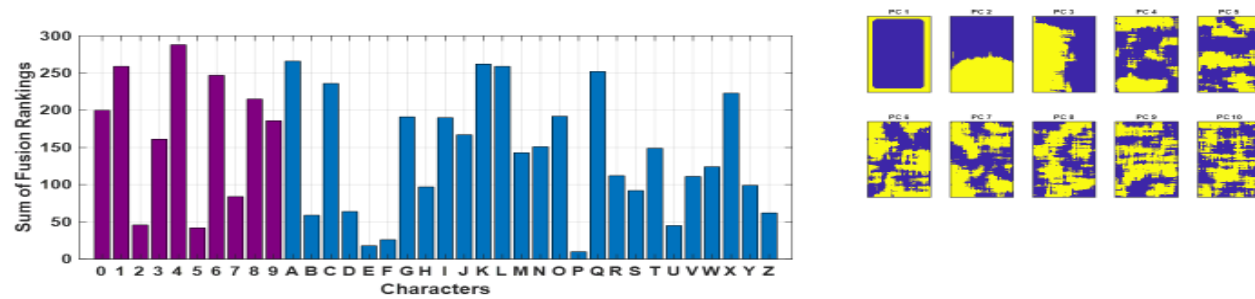


Figure 31. Score images PC1-10 derived from phase images of cycles 51-60 and corresponding character determination by fusion rules.

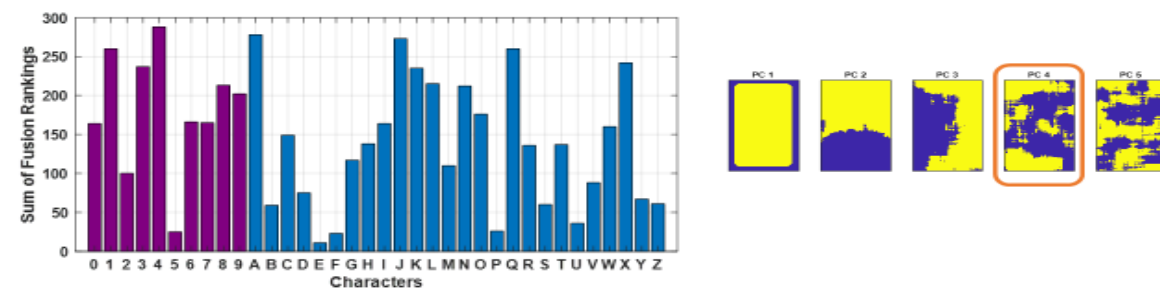


Figure 32. Score images PC1-5 derived from phase images of cycles 56-60 and corresponding character determination by fusion rules.

Note that in general, even with the added alphabetical characters included in the library, the undefaced 2 from the **graded sample** was correctly identified since it had the 1st or 2nd lowest fusion sum ranking until cycles 41-60 or beyond were used. Here the fusion sum ranking became much worse, and this was the case for 46-60 as well. The fusion sum ranking did improve a bit when only 51-60 and 55-60 were used. Since this data was taken for the non-defaced number 2, then the large negative change in the identification for cycles 41-60 and then improvement for 51-60 may be suggestive that there is some drifting in timing of the cycles when several cycles are taken, or that perhaps some of the images contained a significant amount of noise.

The next experiments were performed with a defaced number to determine whether the library match behavior using a single score image derived from various cycles would also be viable when a defaced number was subjected to a similar investigation. The defaced “6” from the **graded sample** was chosen for this. Score image PC5 derived from the various different cycles was picked as the score image to compare with the library. This was based on one person’s observation that the score image PC5 visually looked most like a 6 when accounting for all the cyclic intervals. This seems somewhat arbitrary, but well within the overall goal of the study to see if a single score image or phase image, formed from various combinations of heating cycles, can be used to recover the defaced serial number. The temperature vs cycle number plot for the defaced 6 is given in Figure 33. It was very similar to the temporal plot for the non-defaced number 2. (not shown).

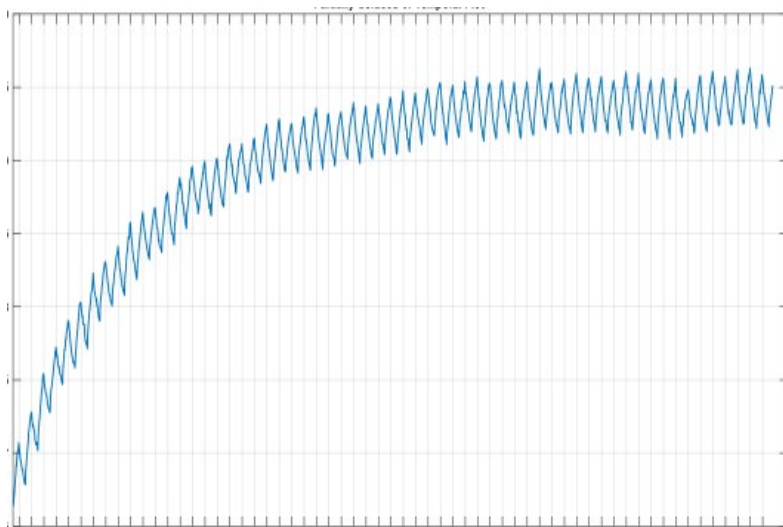


Figure 33. Temporal Profile - Temperature (66.5-70.0) °C vs Lock-in Cycle Number for each of the 61 heating cycles for Defaced 6.

For the non-defaced “2”, increasing the number of cycles included, from 15 to 60, in deriving the score images, modestly improved the ability of the thermal imaging recovery method to determine the identity of the character from the match of score image PC 4 with the library. As can be seen below, Figure 34 shows the score images 1-15 and the corresponding character determination when 15 heat cycles were used to construct the score images for the defaced “6” and using only score image PC5 to match with the library. Comparing this with the results given in Figure 35, when heat cycles 1-60 were used, there was some improvement but both results are fairly poor. The matching algorithm gave an incorrect determination where 23 characters other than the “6” had lower fusion sum values based on matching with score image PC 5 for 15 cycles, and when the number of cycles was increased to 60, the determination was still not correct, but there were only 10 characters with lower fusion sum values than the “6”. If only the numeric characters are considered in the matching, for the 15 cycle case, 3 other numbers (0, 2, and 8) matched better with score image PC5, and for the 60 cycle case 1 other number (0) was a better match.

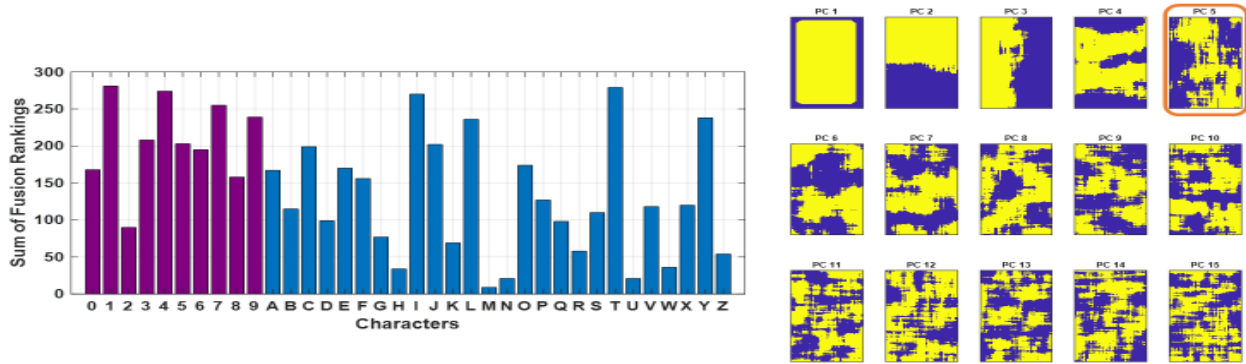


Figure 34. Score images PC1-15 derived from phase images of cycles 1-15 and corresponding character determination by fusion rules.

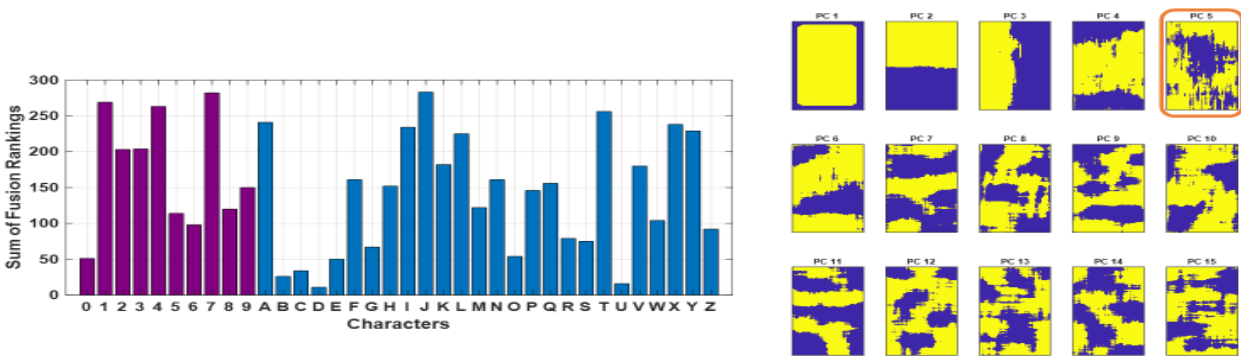


Figure 35. Score images PC1-15 derived from phase images of cycles 1-60 and corresponding character determination by fusion rules.

When the cycles included in creating the score images from the phase images, did not include the first few cycles, for instance if cycles 21-60, or cycles 46-60 were included, the library matching achieved better results. In the 21-60 case, only 5 characters had lower fusion sum values, and for the 46-60 case only 2 characters had lower values. (See Figures 36 and 37). Lastly, as can be seen in Figures 38 and 39, when only the last 10 or 5 cycles were included, the results were very mixed. Including cycles 51-60 to get the score images resulted in 13 characters with lower fusion sum values, and if only cycles 56-60 were included, then the fusion sum value was in fact lowest for the “6”, surprisingly correctly identified the defaced character as a 6. Tests with other defaced numbers showed that this last result was rather serendipitous.

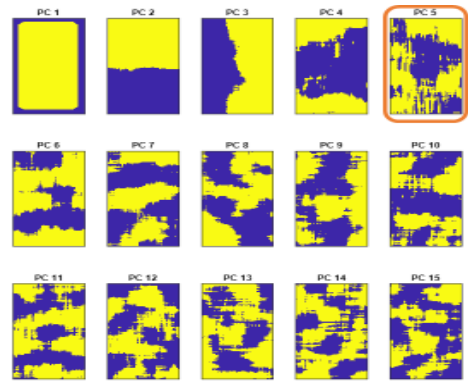
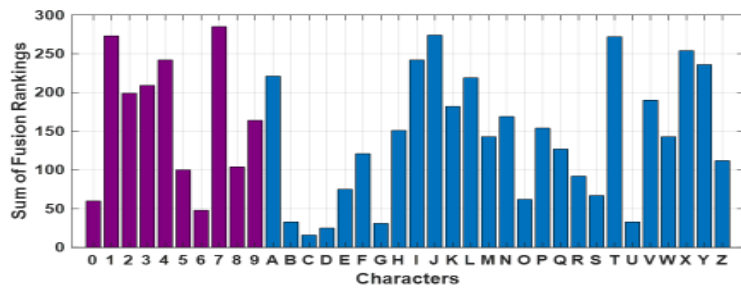


Figure 36. Score images PC1-15 derived from phase images of cycles 21-60 and corresponding character determination by fusion rules.

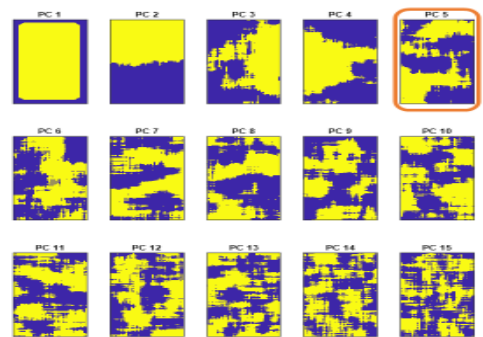
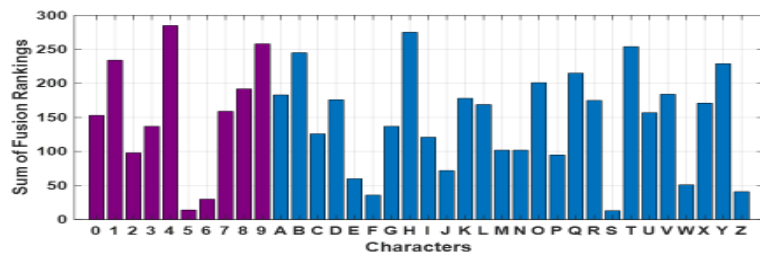


Figure 37. Score images PC1-15 derived from phase images of cycles 46-60 and corresponding character determination by fusion rules.

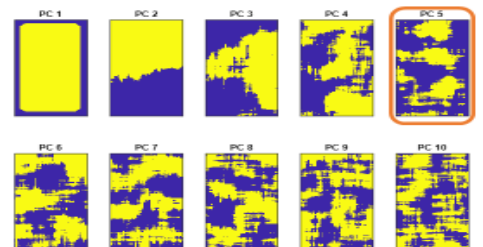
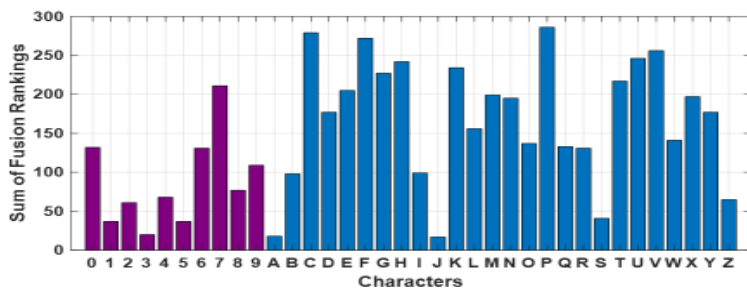


Figure 38. Score images PC1-15 derived from phase images of cycles 51-60 and corresponding character determination by fusion rules.

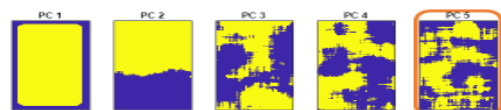
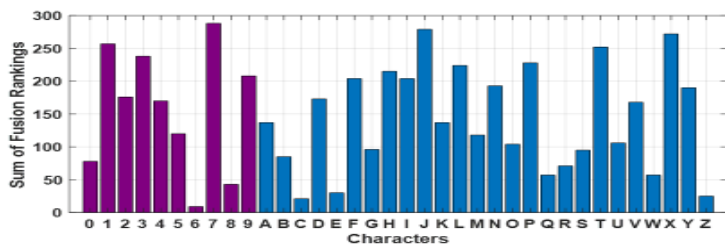


Figure 39. Score images PC1-15 derived from phase images of cycles 56-60 and corresponding character determination by fusion rules.

These tests were aimed at determining the reproducibility of producing a particular score image from phase images derived from both different amounts of cycles used and also for the different numbered cycles. The reproducibility was judged by determining by how well the particular score image chosen, matched with the library to correctly identify the number, either a non-defaced “2” (using PC 4) and then a defaced “6” (using PC 5). The number that produced the best match has the lowest value of the fusion sum. Both visually and through the matching process one finds that there is some variation in the score image for the non-defaced number, and very significant variation in the score image of the defaced number when different amount of cycles and different number cycles are used to produce the score image. **The conclusion is there is a large variability in the score images derived for defaced serial numbers using different heat cycles and numbers of heat cycles.** This variability in the score image results in a significant number of incorrect identifications of a defaced number if only a single score image is used. The small variability in identifying the undefaced number could be caused by noise from inconsistent laser heating of the sample or noise from the environment. Indeed, part of the reason to use the phase images in deriving the score images is the phase images should be less susceptible to environmental noise. As a result of these reproducibility study, the laser was realigned and it was determined that the pulsing circuit was drifting on occasion. This may be related to heating of the components or some drift due to a slight mismatch of the cycle time. An alternative commercial dual pulse system was obtained and replaced the older version.

In addition to investigating whether a single score image with the library matching routine was viable for defaced number recovery an investigation of whether just the phase image itself derived from lock-in thermography of one or multiple heating cycles of the defaced sample could be used to identify the defaced numbers instead of a set of score images. Essentially, the idea is that instead of finding the best match of the pseudo-Zernicke (PZ) moments for a set of score images to the PZ moments in the library, the PZ moments were obtained for the lock-in phase image derived from the camera frames across the laser heat pulse. If after preprocessing the lock-in phase image it somewhat visually resembles a defaced number, then with the appropriate matching routine, a computer identification of the defaced number from the processed phase image should be possible.

To determine the viability of using the phase images in a computerized match, phase images were again obtained for each of the serial numbers engraved on the **graded sample**. As mentioned, for this sample the exact locations and identities of each undefaced and defaced serial number are known. The undefaced two and partly defaced six were used as a cross-reference to locate the approximate section of phase image, which resembles the plastic stain pattern of each serial number. The visual interpretation of phase image associated with undefaced 2 suggests that the small phase values define the features that resemble the stamped region and higher values to non-stamped areas within the image.

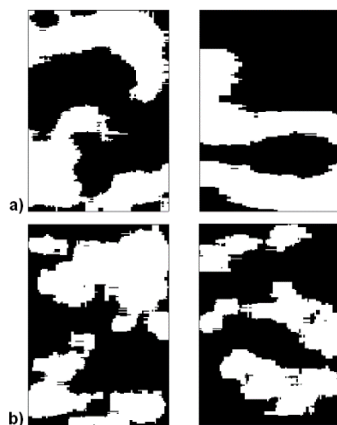
Preprocessing of the phase images was required to convert the phase images to a black and white binary image. It was decided to modify the procedure typically used in binarizing the score images, and create a new procedure to use when forming the black and white phase images. The phase images were converted to binary images using a threshold value. The phase values can be positive or negative. For data transformation, these values were scaled to a fifth power where the positive and negative directionality is still preserved. This transformation was performed to maximize the separation between low and high values so that the distribution is

close to being bimodal. This was done to minimize background noise. An additional step of normalizing the transformed data to a maximum or minimum value ranging from 0 through 1 was performed for consistency with further image processing. A normalized value, close to 0, represents of a non-stamped region, and normalized values close to 1, represent stamped regions.

For binarization, the threshold value was set to be 75th percentile of the pixel values. A foreground pixel value of 1 is assigned to transformed phase image values higher than the threshold and if the transformed values are less than or equal to limit they are assigned a 0. To further improve the quality of the binary image, the image was processed with a smoothing technique called box filtering to reduce background noise. Box filtering involves each pixel value being substituted with the average weight of pixels within the box (17 by 17 pixels) centered on that pixel—image smoothing results in no binarization. Re-binarization of the processed image was done with the threshold of the 50th percentile.

To make the image easier to analyze, image segmentation was applied to simplify the representation of an image into more meaningful images. Image segmentation is the process of partitioning a binary image into multiple segments. For this process, the pixel area with less than the area of box size used for image smoothing is removed so that the unconnected small pixel area does not affect the overall object pattern in an image.

The overall image preprocessing performed on phase image obtained from lock-in thermography for recovery of every defaced serial number was: *Obtain Phase Image -> Undergo Data Transformation and Normalization -> Construct the Binary (Black and White) Image -> Use Box Filtering to Smooth -> Reconstruct the Binary Image after Smoothing -> Perform Image Segmentation -> Result is an Enhanced Binary Image*. The phase image for two replicates was evaluated to recover the undefaced number two and partially defaced six. The location of the phase image that contains the defaced number was known and was consistent with visual inspection of enhanced binary images obtained via image analysis. The size (height and width) of the phase image region containing the defaced number can be tuned with this type of preprocessing until a number or letter pattern is achieved. Then a decision about the identity of the defaced number can be made based on visual inspection of the multiple enhanced binary images obtained using different image sizes and moving to neighboring locations (left to right or top to bottom) about the assumed location. Figure 40 shows binary images developed from the phase shift in the presumed location of the stamped number on a stainless-steel plate. Also included is a repetition of the experiment completed on a different day and after the **graded sample** was remounted under the camera.



required. These can be considered as weak classifiers as some of the information associated with a class could be minimized by averaging, and these classifiers may not be as reliable in classify an image independently.

PLS-DA is a linear classification method that combines the projection-based regression method, partial least squares (PLS) with the discrimination power of a classification technique. PLS finds a linear regression model with a maximum covariance between the dependent and independent variables. The linear regression models are called latent variables (LVs) that are the linear combination of independent variables. Hence, the tuning parameters of PLS-DA are LVs (1,2, 3... full rank), which describes the appropriate sources of data variability. PLS1-DA is applied for one dependent variable (y) and PLS2-DA for multiple independent variables (Y). These response variables are replaced by the set of dummy variables describing the categories that express the class membership of the statistical units. This constraint does not allow for other response variables than the one for defining the types of images. As a consequence, all independent variables play the same role for the class assignment.

PLS-DA is performed to sharpen the separation between groups of observations, by selecting LVs such that a maximum separation among classes is obtained to understand which tuning parameter carries the class separating information. The efficiency of the method is dataset dependent. An illustration of enlarged separation between two types PCA and PLS-DA is shown in Figure 41 for classification at a specific number of LVs.⁸

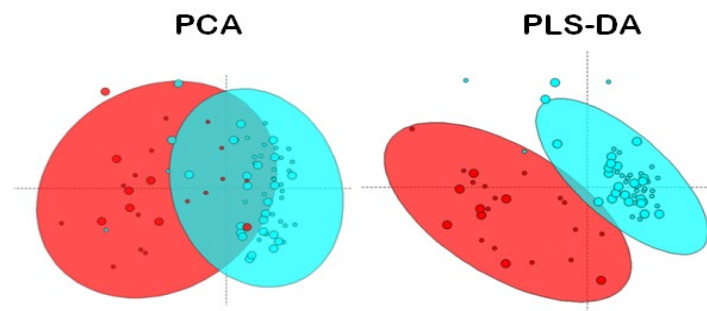


Figure 41. Classification using PCA and PLS-DA.⁸

The kNN is a non-parametric classification method based on distance measures, such as Manhattan, Chebyshev, and Euclidean distance. An object is classified by a majority vote of its k neighbors, with the purpose assigned to the class most common among its k nearest neighbors. Figure 42 demonstrates a schematic diagram of the kNN classification.⁹

The number of neighbors (k) is the parameter used for kNN classification. The distance is measured between the independent variables of each training sample and a new sample. The most commonly used distance measure is the Euclidean distance. It can be observed in Figure 42

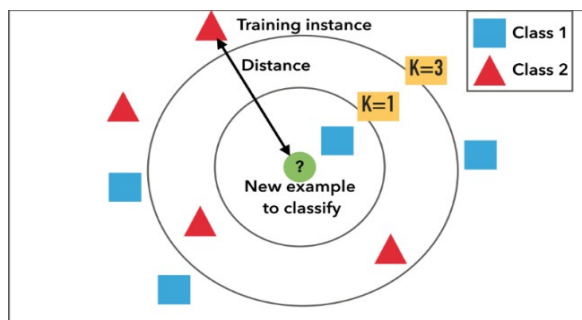


Figure 42. An example of kNN classification.⁹

that depending on the value of k ; the object can be classified either way. This problem demands optimization of the tuning parameter.

Fusion tends to strengthen the classification compared to a single classifier since the outcome is based on diverse information provided by multiple classifiers. There are three approaches to fuse classifiers. One of the strategies uses a separate algorithm such as random forests and other bagging processes to come up with a set of classifiers. The purpose of this approach is to combine weak classifiers to form reliable classifiers. This fusion method still requires method selection and optimization of the tuning parameter. The second approach is to combine optimized classifiers, which is more efficient, as this fusion strategy avoids choosing a single method for classification. However, this still requires picking a set of classifiers and the best single tuning parameter for each classifier. The third approach is to ensemble non-optimized classifiers with tuning parameter window. Rather than selecting an individual tuning parameter, windows of tuning parameters are used. For example, with PLS-DA, the LVs are 1,2,3,..., p where p is the total number of LVs used, and windows of LVs are 1,1-2, 1-3, 1-4,...,1- p . This approach makes it possible to avoid both method and tuning parameter selection for robust classification.

Fusion classification involves defining reference classes, non-optimized classifiers, and fusion processes. Thirty-six classes of pre-defined alphanumeric characters (0-9 and A-Z) are studied. Thirteen classifiers, including six of them with tuning parameter windows and rest with no tuning parameter, are used. A sum fusion rule is used to combine classifiers with a fixed set of tuning parameter window at each object's proportion independently. The sum fusion rule is applied across row normalized classifier values for each alphanumeric class. The number or a letter with the lowest sum value (lowest ranking) will be identified as a defaced serial number. For consensus identification, the majority vote of fusion outcomes among three different object proportions (35%, 50%, and 65%) is used to finalize the classification.

In this study the reference classes are the binary images of thirty-six alphanumeric characters (0-9 and A-Z) derived from Microsoft fonts are used. Twenty-five different fonts were used as instances for individual categories of numbers and letters. The Microsoft font names were Gungsuh, Franklin Gothic Book, Segoe UI Black, Cambria Math, Arial, New Gothic MT, Abadi, Agency FB, Bahnschrift, Bookman Old Style, Baskerville Old Face, Bauhaus, Bernard MT Conc, Bodoni MT Posted, Bodoni MT, Rockwell, Comic Sans MS, Segoe Print, Showcard Gothic, Wide Latin, Goudy Stout, Cooper Black, OCRB, Biome, and Niagara Gold. Two font styles, regular and italics, for each font are included in a class. Thus, each class contains fifty representation vectors associated with the fonts and their styles.

A total of thirteen classifiers are used to identify into which class the phase image should belong, 6 tunable classes (PLS-DA, kNN, Mahalanobis Distances (MD), $\sin \beta$, Q-res, and Divergence Criterion (DC) and 7 non-tunable similarity merits (Cosine, Euclidean Distance, Determinant, Constrained Procrustes Analysis, Unconstrained Procrustes Analysis). Each of the thirteen classifiers is used to compare pseudo-Zernicke moments of the phase image, and the moments of the library and classify it into one of the thirty-six alphanumeric classes. For those six classifiers with tuning parameters, the phase image PZ moment comparison is performed accounting for all of the 45 tuning parameters. Fusion is then carried out using all thirteen classifiers. The sum fusion rule is the most commonly used fusion process for classification. The fixed tuning parameter window size close or equal to full rank is applied to avoid tuning parameter selection. The window size of forty-five is selected based on the minimum across full rank for each class used in eigenvector-based classifiers. The number of nearest neighbors for

kNN is the same as the tuning parameter window used for eigenvector-based classifiers. Before fusion, classifier values were row normalized to unit length in order to eliminate magnitude differences between the classifiers. The normalized row values are summed for each class, and the class with the lowest sum value is the classified number or letter. Each tuning parameter window for tuning parameter-based classifiers has the same contribution as the individual similarity measures in the fusion process. For each object proportion, the same window size is used for eigenvector-based classifiers. Figure 43 shows the normalized raw values of six tuning parameter-based classifiers at each window and SM along with sum fusion value for identification of phase image associated with undefaced 2.

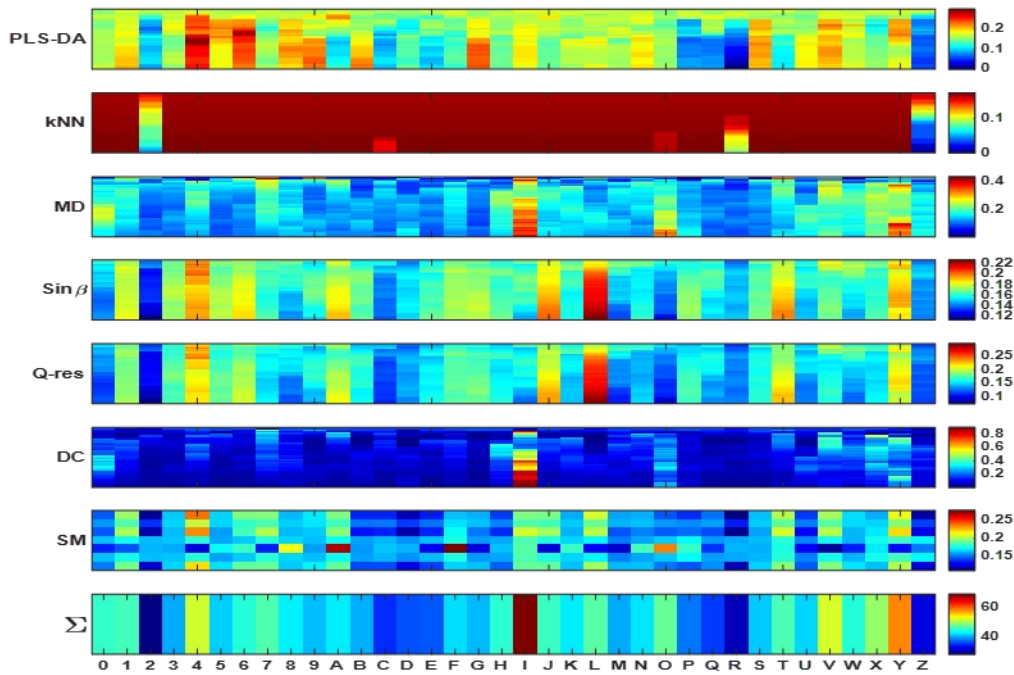


Figure 43. Fusion Classification input matrix and sum fusion value (undefaced 2- first replicate) with RM of a specific proportion (35%) and tuning parameter window size of forty-five.

In Figure 43, for Classification of the lock-in phase image of the undefaced 2, the dark blue color represents the lowest classifier value (red is the highest) and best match of the phase image to that particular alphanumeric class. With the exception of the kNN classifier, a blue or dark blue color appears for the classifiers and across the tuning parameters for those classifiers with tuning parameters. Also, the sum, Σ , at the bottom of the figure, shows that the sum fusion is minimal for the alphanumeric class 2, and so the undefaced 2 is classified as a 2. This information is also represented in Figure 44, where an additional preprocessing step of expanding the proportion by 50%. Note that other characters (S and Z) also had fairly low values of the sum fusion, and in fact at different dilation percentages, their sums were slightly below the sum for the 2. This will be discussed more fully in the next section of this report.

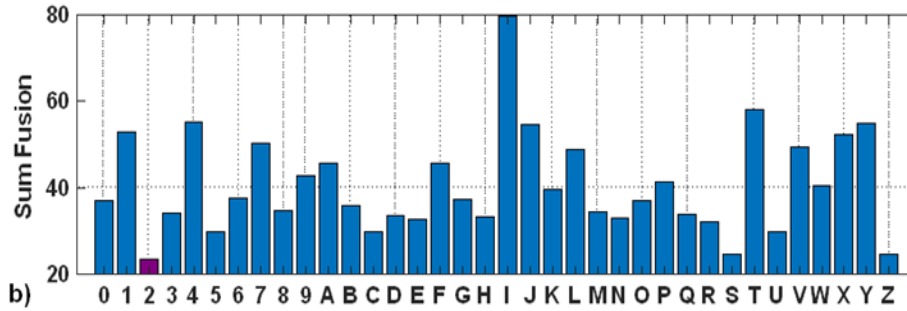


Figure 44. Bar plot of Classification Sum Fusion for first replicate of undefaced two with PZM at 50% dilation of the phase image. The magenta color bar represents the lowest sum fusion value (lowest rank)

The classification of the lock-in phase image of the defaced 6 also yielded favorable results as shown in figure 45. In the case of the defaced 6, its classifier sum was significantly lower than any of the other sums.

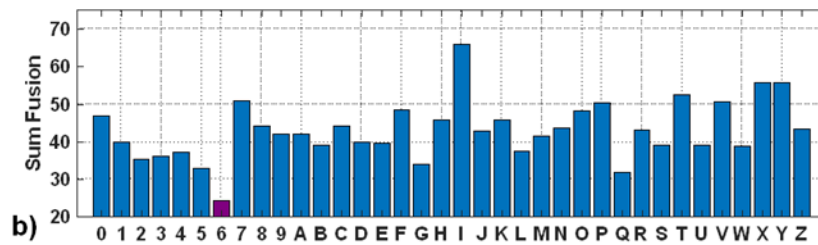


Figure 45. Bar plot of Classification Sum Fusion for partially defaced six at 50% dilation of the phase image. The magenta color bars represent the lowest sum fusion value (lowest rank)

Based on these two results, **use of the enhanced binary phase image, derived from lock-in thermography at an optimized frequency, in combination with Classification Testing** is a viable technique for determining the identity of a defaced number. This technique, the automatic character identification protocol method, (ACIP), was developed by Anit Gurung, the Master’s student who worked on this project. It is the focus of his Master’s thesis which is included as an attachment with this final report.

The ACIP method was also applied to other samples, the defaced characters on the gun barrel, and the defaced characters on the laser engraved forceps. As with the **graded sample**, the approximate positions of the characters and the character’s identity are both known. The results of comparing PZ moments of enhanced binary phase image to the library using the *Classification* comparison method for the gun barrel and the needle handler (forceps) are given here. Note that in these studies the PZ moments were modified to be sensitive to rotational variance in the images. This will be discussed more thoroughly in the next section of the report.

There were two defaced numbers on the shotgun barrel sample. As can be seen from the before defacing and after defacing pictures shown in Figure 46.



Figure 46. Picture of Shotgun before and after the model number was defaced.

The first number was a 1 and the second a 2. A lock-in frequency of 1.5Hz was used to create the phase image. Next, the pattern recognition method (ACIP) was applied in the following way. The image was reprocessed to produce the enhanced binary image which was also dilated by 50%. The PZ moments were then derived for that image and these moments were compared with the library using the *Classification* comparison method. The results of applying ACIP to this defaced number on the shotgun barrel are shown in Figure 47. In this case defaced number was correctly identified by comparing the enhanced binary phase image PZ moments to those in the library.

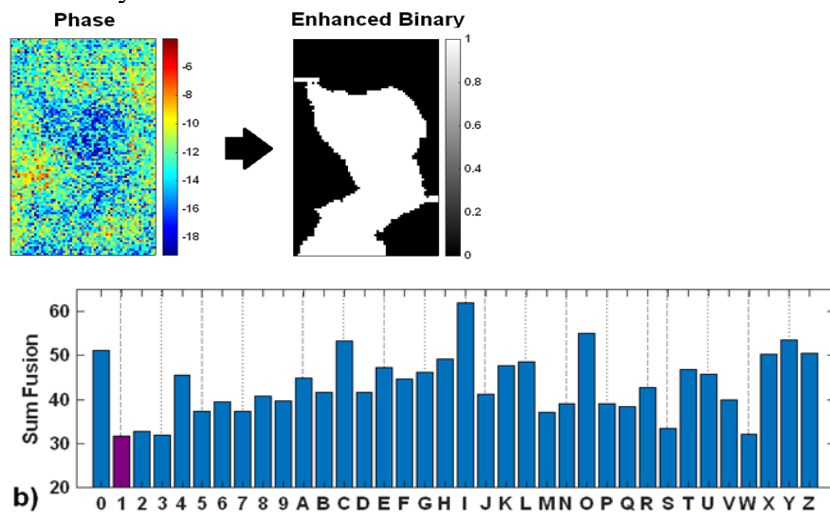


Figure 47. Phase and Enhanced Binary images of defaced 1 on the shotgun barrel. Also shown is the Sum Fusion for identifying the character using the *Classification* comparison method.

The ACIP method was also used to identify the second defaced number, the number 2. All the experimental parameters in this experiment were the same as those used for the defaced 1. The results of this are shown in Figure 48.

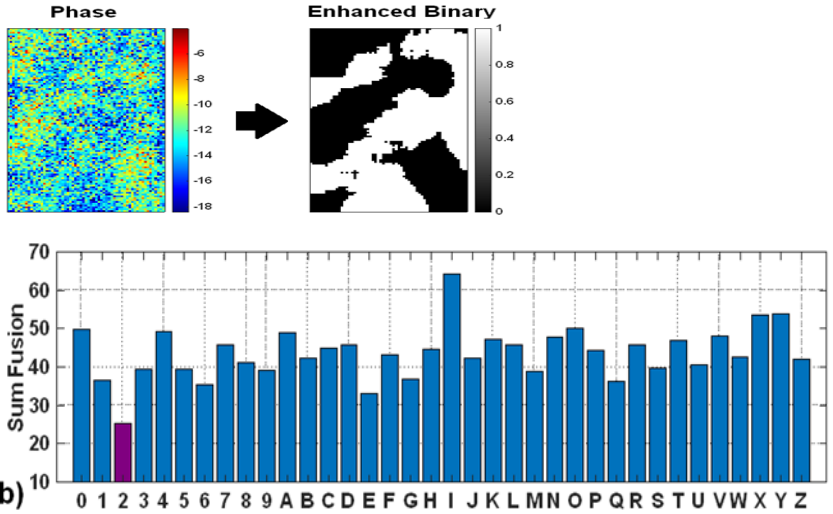


Figure 48. Phase and Enhanced Binary images of defaced 2 on the shotgun barrel. Also shown is the Sum Fusion for identifying the character using the *Classification* comparison method.

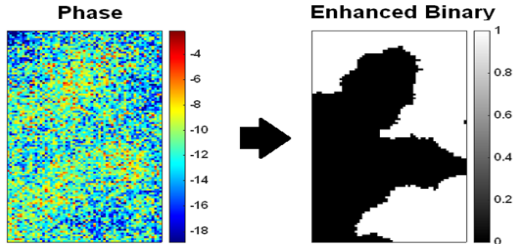
The results look promising as both of the defaced numbers on the shotgun barrel were correctly identified.

Essentially the same comparison procedure was applied to the defaced 3 and defaced 4 on the forceps. The picture of the laser-engraved number before and after it was defaced is provided in Figure 49.



Figure 49. Picture of Forceps before and after the serial number was defaced.

The results of using the ACIP method to identify the defaced numbers on the forceps are given in Figure 50 and Figure 51.



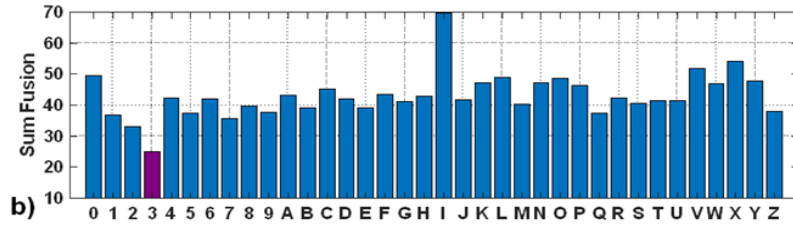


Figure 50. Phase and Enhanced Binary images of defaced 3 on the Forceps (Needle Holder). Also shown is the Sum Fusion for identifying the character using the Classification comparison method.

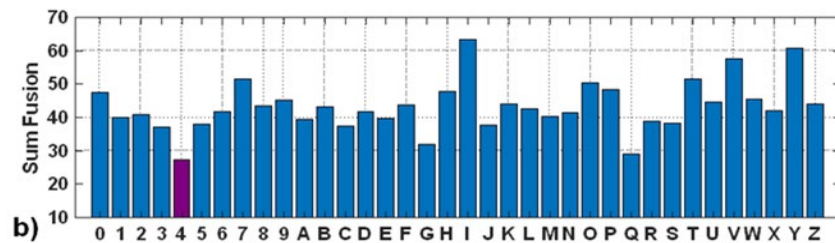
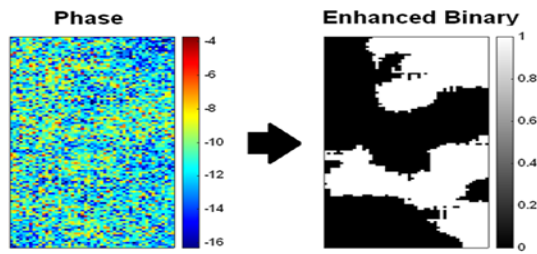


Figure 51. Phase and Enhanced Binary images of defaced 4 on the Forceps (Needle Holder). Also shown is the Sum Fusion for identifying the character using the Classification comparison method.

Again the results look very promising since both the defaced 3 and defaced 4 were successfully identified using the *Classification* method. One important point to note is that the location and actual identity of the defaced number were known by the experimentalist. A replicate was performed on the **graded sample**.

Summarizing the results from this section of the report, it appears that *Library Matching* of the pseudo-Zernicke moments of a single score image, from the many that can be generated by PCA of the thermal lock-in phase image, with the pseudo-Zernicke moment of the library does correctly identify the **undefaced** number. Generally, the more heating cycles that are used the better the match, and the use of particular subsets of the total cycles did not provide a significant affect either way. **However**, when a single score image of a **defaced number** is used for the library matching, it was found that the computerized Library Matching did not successfully identify the defaced number. Lastly, in some studies spearheaded by Master of Science candidate, Anit Gurung, use of the enhanced binary phase image, rather than a score image, did provide the correct identification of the defaced number if the comparison method to the moments of the enhanced plasma image involved classifying the image into one of the 36 alphanumeric classes through a library comparison method known as Classification.

IIC. Similarity Merits

An important part of the computer determination of the serial number depends on the calculation of the similarity merits and optimization of the character fonts used in the number comparison library. One of the most significant steps in assigning the similarity merits is to first represent the number library images, and the enhanced binary PCA score images or the enhanced binary phase images, in terms of the Zernike or pseudo Zernike moment vectors. In addition to obtaining the enhanced binary score or phase images through the binarization procedure described in the previous section, important considerations for optimization of this process to obtain the best similarity measures are:

- 1) Is it important to enlarge or shrink the score images to match the library image sizes, and how is this best done? Is image dilation helpful in identifying the defaced serial number through the either the Library Matching Comparison Method and/or the Classification Method?
 - 2) Is the rotational invariance of the Zernike and pseudo-Zernike (PZ) polynomials and moments helpful in matching score images to the number library images? Would it be better to have PZ-like polynomials that are sensitive to the relative rotational orientation of the images?
- Studies of the effect of both dilation and also using rotationally variant Zernicke polynomials and moments to represent the score and/or phase images and the library images were investigated.

Dilation Effects

In taking the data, there is often a difference in the score images derived from the thermal imaging, in comparison to the numbers in the library. One would expect this size difference to have a significant effect on assigning the similarity merits. An example of a typical size difference that might be encountered between the score image and library font character is shown in Figure 52.

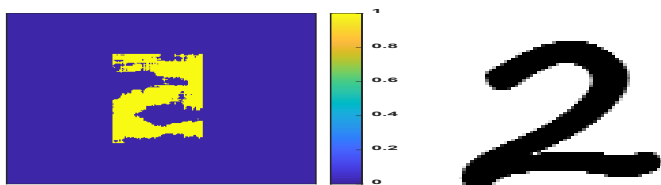


Figure 52. Score Image of a Defaced 2 compared with a Segoe 2 from the number library.

Note that in the score image of the defaced 2 there is a significant amount of boundary area which is blue colored, containing no part of the score image, whereas the 2 in the number library image has a minimal amount of boundary area. One can "dilate" or enlarge the image by using a smaller pixel area for the score image.

Without enlarging the number and reducing the boundary area a comparison of the undilated score image with the images in the library results in an incorrect identification of the score image as a B, R, or 5. (See Figure 53). Note that capital letters have been included as part of the library images. There are several fonts included in the library images, and the best match is determined by the character with the lowest value of the sum of the fusion rankings derived from the similarity measures.

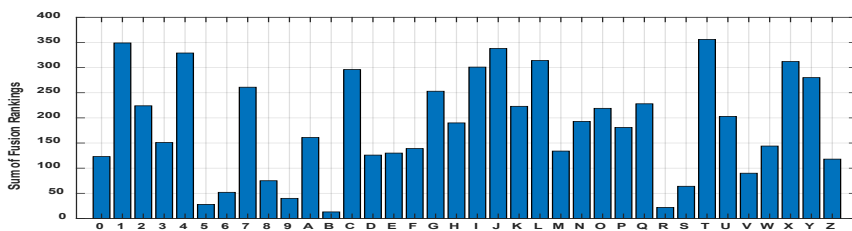


Figure 53. Comparison of the undilated score image to multifont image library

If one "dilates" the number (see Figure 54 below) by using a smaller pixel areas for the image containing less and less of the boundary area, the similarity merits improve and the fusion rules show an improvement in selection of the correct number.

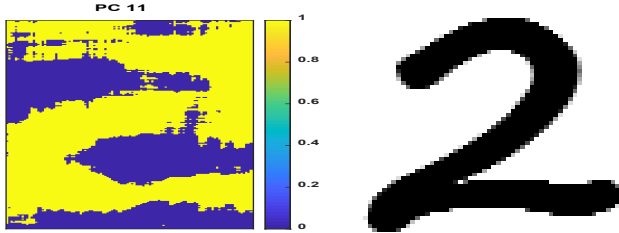


Figure 54. 201 x 111 Pixel Dilated Score Image for comparison with Segoe library font image

If one dilates the image and uses the Segoe font in the number library for comparison purposes then the identification of the defaced image improves significantly as seen in the bar charts below in Figure 55.

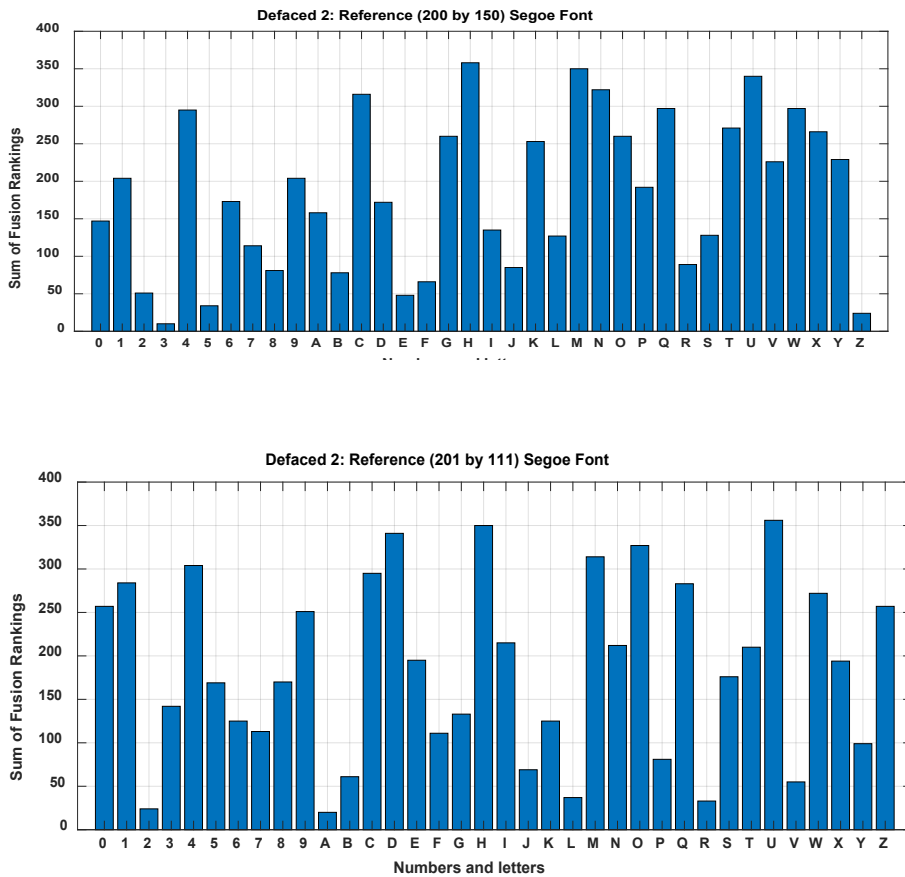


Figure 55. Successive Dilation of the Score image for comparison with the number 2 from the Segoe font. Identification of the defaced image as a number 2 is much improved.

After performing an initial dilation of the images, and using only the Segoe font in the number library, the best match to the image of the defaced number is a "3", "Z" or "5". The correct match of the "2" is not in the top 3 choices. After performing increased dilation, the "A" and "2" have the lowest sum of the fusion rankings indicating that the defaced number is likely an A or a 2.

Dilation or erosion also has an effect in identification of the number using a *Classification* method as in the ACIP method described previously. A dilation factor of 35%, 50%, and 65% were applied to enhanced phase images as described here, and then the effect of the dilation on the success of identifying the number was determined. The phase and reference binary images ($x \times y$ pixels) are resized to a fixed dimension (200×100) for consistency across all images. The boundary of the object pattern in the binary image is enlarged using dilation and reduced with erosion. With dilation, additional features are added to the boundary of the object, and with erosion, the existing feature at the object boundary is removed. The morphological operations, such as dilation and erosion, are applied to the enhanced binary image to form an image with desired object proportion. Three different proportion, 35%, 50%, and 65%, were chosen based on their ability to retain the original pattern of the image with minimal variation consistently, as shown in Figure 56.



Figure 56. An example of morphological operations performed on binary image converged to different object area percentage a) 35% b) 50% and c) 65%

Mapping the image residing in a unit circle with the origin at the center of the image is required to evaluate the Pseudo-Zernike moments. Pixels outside a unit circle are not used in computing the moments. Thus, to ensure that all phases and library image pixels are captured within the unit circle, each binary image is placed into the square image of dimensions calculated by

$$N_x = N_y = 2\sqrt{n_x^2 + n_y^2}$$

where:

n_x and n_y are respectively one half of the number of x and y pixels in the image, and N_x and N_y are the new dimensions of the resized image.

This dilation method was applied to the defaced model number on the shotgun barrel and also the defaced laser engraved serial number on the forceps. The bar graphs in Figure 57 and Figure 58 show the effect of using different dilations on the enhanced binary image when using the *Classification* procedure in attempting to find the best match of the enhanced binary phase image to the library. In Figure 56 if the object percentage is smaller in the 35% and 50% ranges, then the number matches well, but if the object percentage is 65%, then the defaced number is

incorrectly identified as a W, and S, D, 2 and 3, also have lower sum fusion values than the correct number, the number 1.

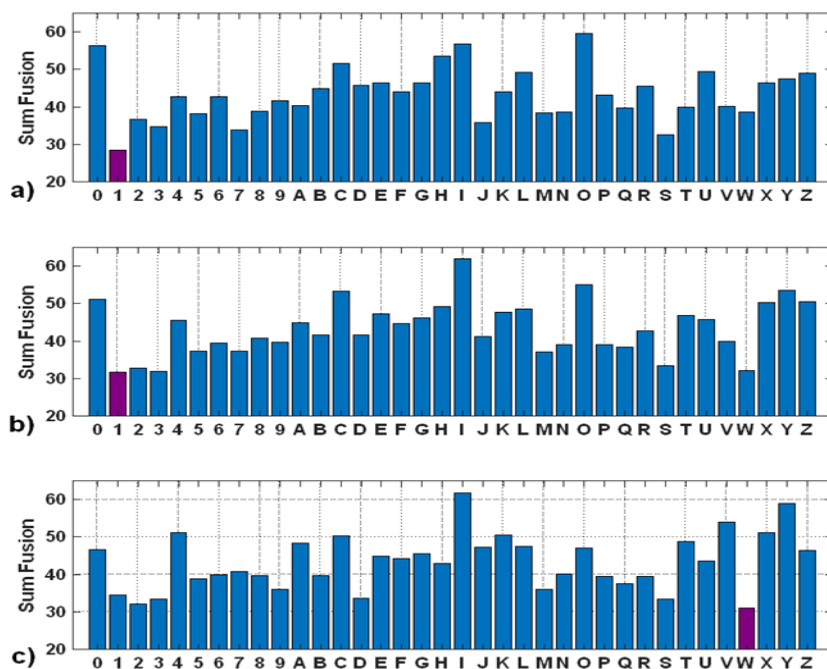


Figure 57. Bar plot of Sum Fusion for defaced 1 on the shotgun barrel with dilation by varying object percentage a) 35%, b) 50% and c) 65%. The magenta color bars represent the lowest sum fusion value.

However, as can be seen below in Figure 57, at all dilation values, the number is correctly identified as a 2, and the dilation appears to improve the delineation between the correctly identified 2 and the next closest alphanumeric character.

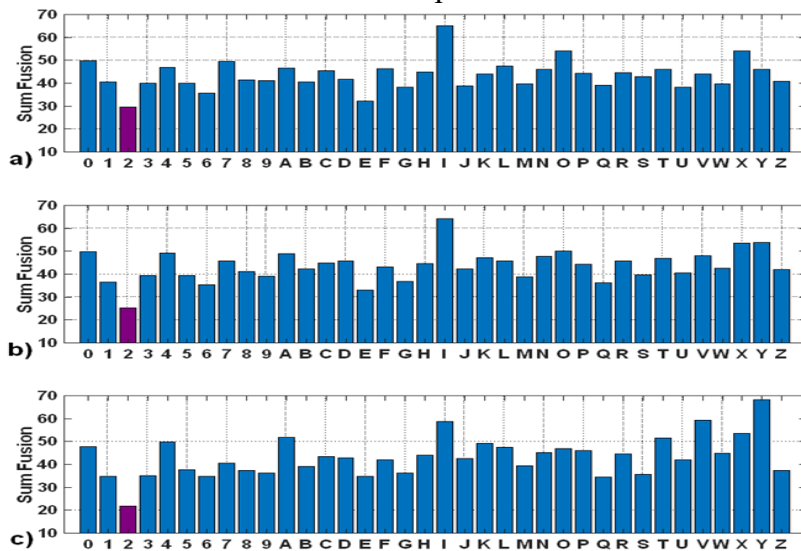


Figure 58. Bar plot of Sum Fusion for defaced 2 on the shotgun barrel with dilation by varying object percentage a) 35%, b) 50% and c) 65%. The magenta color bars represent the lowest sum fusion value.

A similar dilation experiment was performed with the laser engraved serial number on the forceps (needle holder) for the defaced 3 and defaced 4. Here again, then object percentage was varied from 35% to 65%. The bar graphs in Figure 59 and Figure 60 show the effect of using different dilations on the enhanced binary image when using the *Classification* procedure in attempting to find the best match of the enhanced binary phase image to the library.

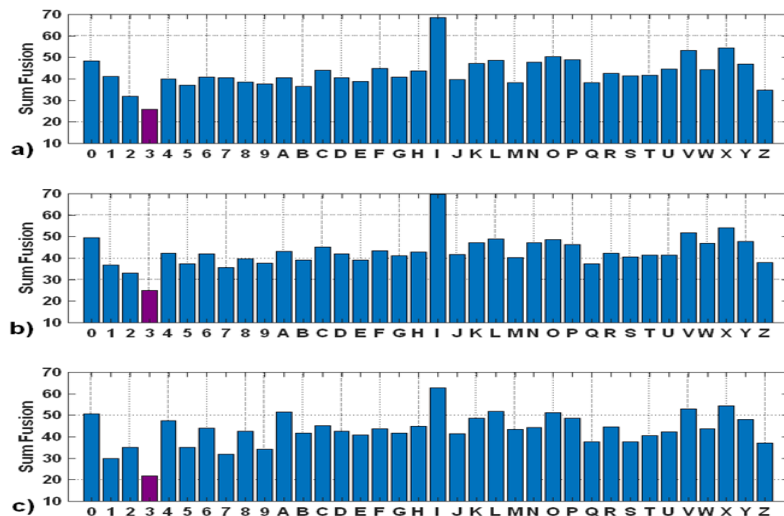


Figure 59. Bar plot of Sum Fusion for defaced 3 on the forceps (needle holder) with dilation by varying object percentage a) 35%, b) 50% and c) 65%. The magenta color bars represent the lowest sum fusion value.

As can be seen in Figure 59, at all dilation values, the number is correctly identified as a 3, and the dilation appears to improve the delineation between the correctly identified 3 and the next closest alphanumeric character. However, as can be seen in Figure 60, use of the *Classification* method correctly identified the defaced 4 only dilation at the higher object percentages of 50% and 65%

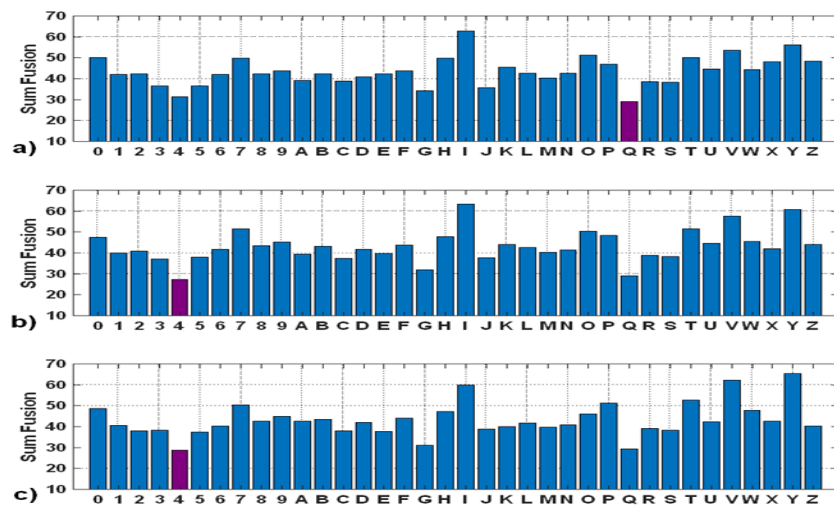


Figure 60. Bar plot of Sum Fusion for defaced 4 on the forceps with dilation by varying object percentage a) 35%, b) 50% and c) 65%. The magenta color bars represent the lowest sum fusion value.

In summary, dilation by varying the object percentage can have a large effect on use of the Similarity Merits in identifying the defaced serial number. Note that use of larger dilation values, does not always improve the ability of the image matching procedure to determine the identity of the defaced number. The best use of dilation is probably to perform 3-4 dilations and matching procedures, and then fuse these results with one another.

Effect of Allowing for Rotational Variance

The effect of using pseudo-Zernicke moments that are independent of image rotation or other moments that are sensitive to the rotational orientation of the object was also examined. on the ability of the similarity measurements and fusion rules to correctly identify the defaced serial number. The expressions for the Zernike and pseudo Zernike moment vectors contain an exponential part that makes them rotationally invariant, or said another way allows for the Zernike moment images to rotate freely when performing the similarity merit comparisons and ultimately in calculating the best match by the fusion rules. One can imagine that rotational invariance could be neutral, helpful, or detrimental to correct identification of the defaced number in some cases. For example, in the score image of the defaced number shown previously, if the number is rotated in the plane of the page by 180° (see figure 61 below), then it then it still looks like it could be a number "2", and so if the score image was somehow rotated relative to the number library, then it would not matter too much.

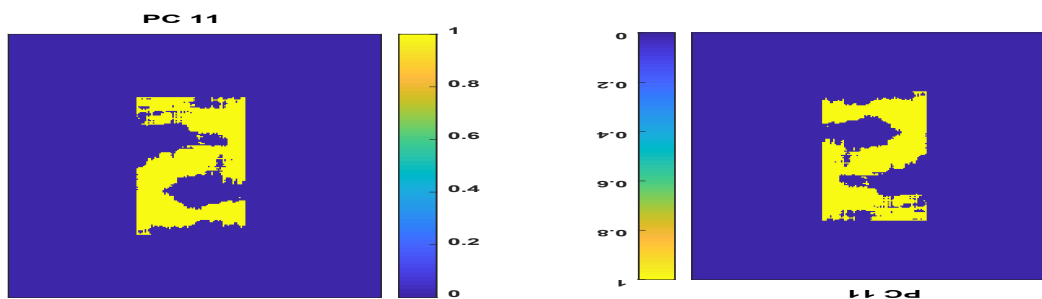


Figure 61. Score image of the Defaced 2 and the score image rotated by 180°

However, in other cases, rotation of the image may lead to a false identification as one could imagine from Figure 62. The first image in figure 6 is a score image of a defaced number 6, and the second image is that score image rotated by 180° in the plane of the page. The first image might likely be identified as a "6" or perhaps a "G", whereas the rotated image looks more like a "9" or perhaps a "3".

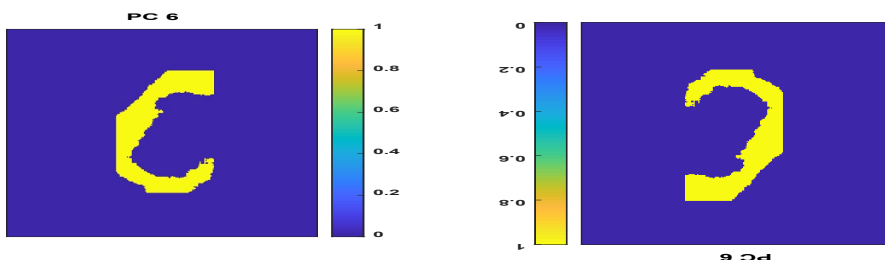


Figure 62. Score image of the Defaced 6 and the score image rotated by 180°

To investigate the effect of rotational invariance on the correct identification of a defaced number we performed similarity measures with Zernike moments that included the rotational invariance exponential factor and then performed the similarity measures where the invariance was negated. The ones where the rotational invariance is negated are called rotational variants and are known as Radial moments or RM. In the bar graphs presented below, (see Figures 63 and 64), the defaced number 6 was compared with the Gungsoh font as the number library using rotationally invariant pseudo-Zernike moments (PZM) and when using rotationally variant moments (RM). Again in the rotationally variant moments, the RM, are sensitive to the rotational orientation of the object.

Note that in both cases the images were dilated. For the defaced number 6, use of the rotationally variant (RM) moments, in the older Library Matching procedure provided the "6" as the 2nd best match for the defaced 6 (Z was the best match), and when using the PZ moments, here too the "6" was identified as the second best match behind the C. Here, use of moments that were rotationally variant or invariant did not largely affect the degree of correct identification, although the best match was different.

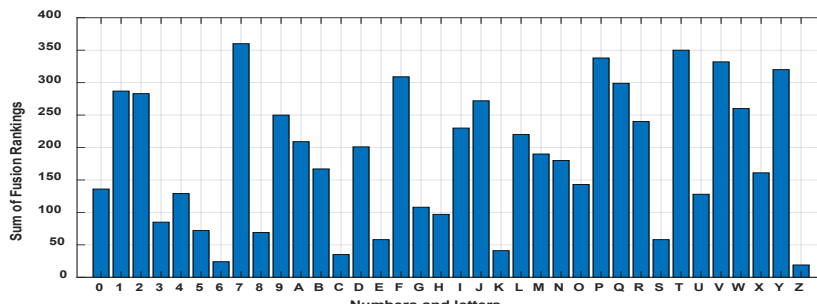


Figure 63. Ranking for Defaced 6 w/Dilation and the rotationally variant RM moments.

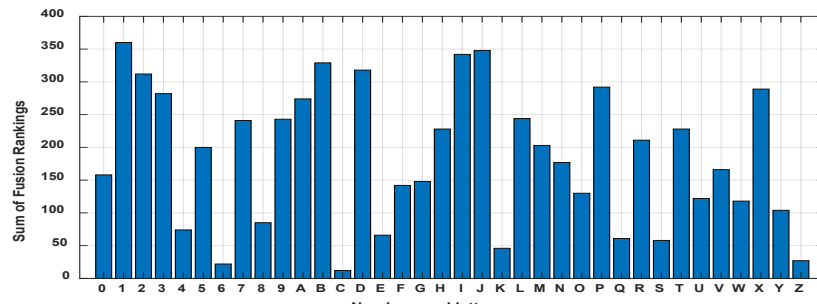


Figure 64. Ranking for Defaced 6 w/Dilation and the rotationally invariant PZM moments.

However, as seen in Figure 65 and Figure 66, in the case of a defaced number 5, when rotation was denied, the defaced image was correctly identified as a "5". When rotation was allowed the best match was with a "Q" followed by a "C" and then an "O". The number "5" was the 4th best match. Here the rotational invariance resulted in a more significant change. One should note, however that the library contained only one type of font, the Gungsoh font, and perhaps the results would have been different if another font had been chosen for the library or if a number of fonts had been chosen for the library.

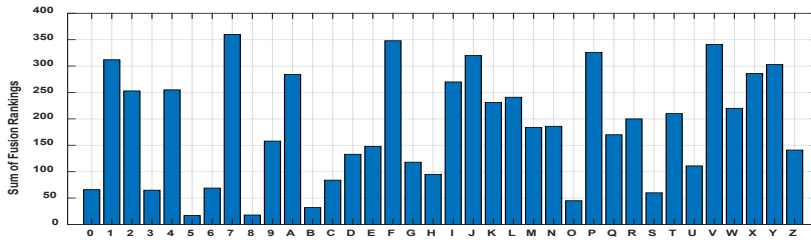


Figure 65. Ranking for defaced 5 w/dilation and the rotationally variant RM moments.

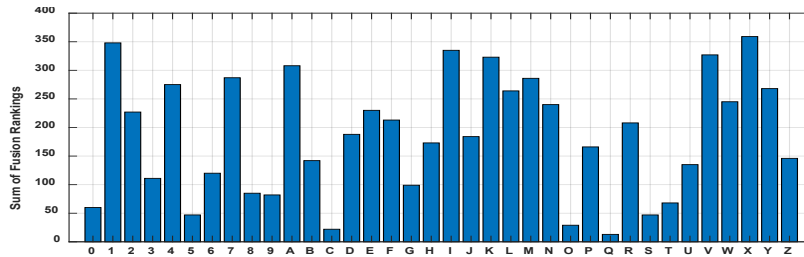


Figure 66. Ranking for defaced 5 w/dilation and the rotationally invariant PZM moments.

A similar result was found using the ACIP method with matching to the library provided through the *Classification* method rather than the typical Library Matching procedure. The difference in identification of the undefaced 2 on the **graded sample** using RM vs PZM moments is given in Figure 67 and Figure 68.

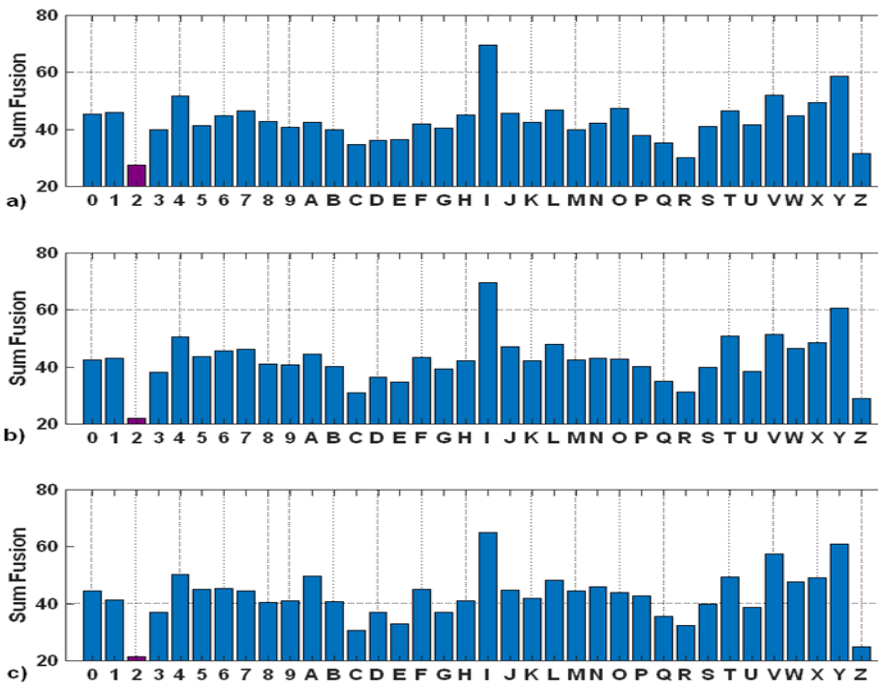


Figure 67. Bar plot of Sum Fusion for first replicate of undefaced 2 with RM and varying object percentage a) 35%, b) 50% and c) 65%. The magenta color bar represents the lowest sum fusion value.

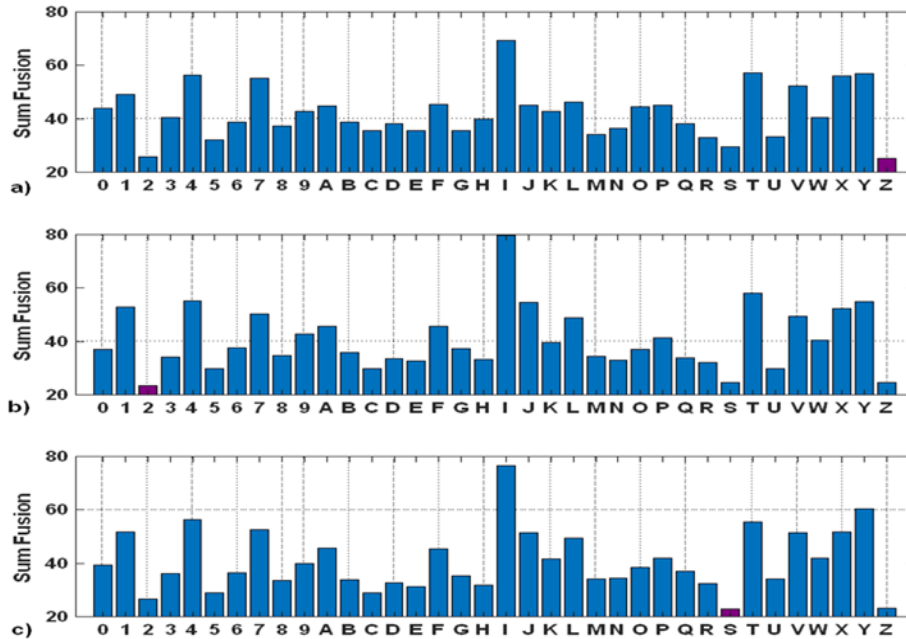


Figure 68. Bar plot of Sum Fusion for first replicate of undefaced 2 with PZM and varying object percentage a) 35%, b) 50% and c) 65%. The magenta color bar represents the lowest sum fusion value.

With RM, the fusion classification identifies the serial number accurately for all three different proportions. The serial number was correctly identified with the absolute majority. However, using PZM, only the image with 50% proportion is identified correctly.

In summary, based on the experiments with the defaced six using Library Matching and with the undefaced 2 using *Classification*, it was observed that better identification of alphanumeric characters is possible using the RM moments. These are the rotationally variant moments and are sensitive to the rotational orientation of the object of interest.

IID. Libraries and Computer Matching Algorithms

Another aim of this work was to better define how to choose fonts that should be included in the number library and how many sets of character fonts should be included. This essentially involved investigating how the comparison by similarity measures and fusion rules was affected by using one font in the numerical library or several common fonts. For the previous grant we used 10 font types in the numerical comparison library, and here we investigate how the identification of the defaced number is affected by using only a single font. For this study we chose the fonts:

- | | |
|---------------------------|----------------------------|
| Times New Roman (normal) | Times New Roman (italics) |
| Tempus | Segoe Pring |
| Gungsuh (normal) | (Gungsuh (italics) |
| Arial Rounded MT (normal) | Arian Rounded MT (italics) |
| Arial Black (normal) | Arial Black (italics) |

Each font was individually used as the numerical comparison library and the ability for each library to correctly identify the defaced 6 and the defaced 5 is given in Figure 69 and Figure 70 respectively.

Microsoft Fonts and Defaced 6

1. Times New Roman (Normal)
2. Times New Roman (Italics)
3. Tempus
4. Segoe Print
5. Gungsuh (Normal)
6. Gungsuh (Italics)
7. Arial Rounded MT (Normal)
8. Arial Rounded MT (Italics)
9. Arial Black (Normal)
10. Arial Black (Italics)

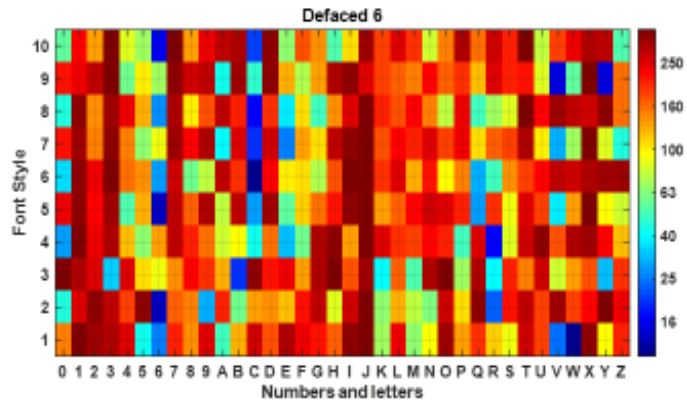


Figure 69. Capability of individual fonts to identify the defaced number as a 6. (Note that the Dark blue color indicates the best fit and red is the worst fit.) Here the Times New Roman (italics), Gungsuh (Normal), and Arial Black (italics) indicated that the best fit was a number 6.

Microsoft Fonts and Defaced 5

1. Times New Roman (Normal)
2. Times New Roman (Italics)
3. Tempus
4. Segoe Print
5. Gungsuh (Normal)
6. Gungsuh (Italics)
7. Arial Rounded MT (Normal)
8. Arial Rounded MT (Italics)
9. Arial Black (Normal)
10. Arial Black (Italics)

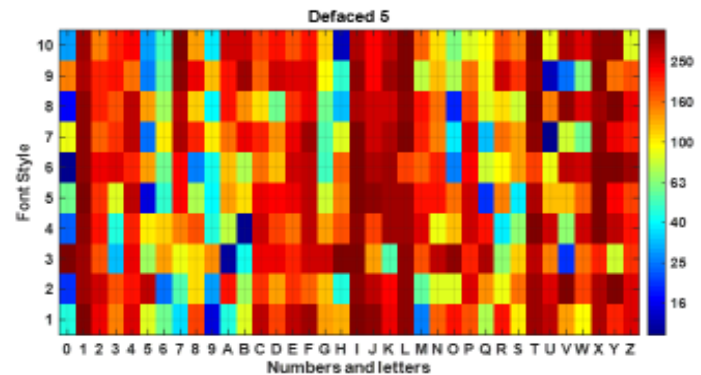


Figure 70. Capability of individual fonts to identify the defaced number as a 5. (Note that the Dark blue color indicates the best fit and red is the worst fit.) Here the Gungsuh (Normal) font indicated that the best fit was a number 5.

Based on these results, it appears that some fonts contribute more to the correct identification of the defaced serial number than others. For the defaced 6, the Times New Roman (italics), Gungsuh (Normal), and Arial Black (italics) indicated the best fit was a 6, and the Times New Roman (normal), Gungsuh (Italics) and Arial Rounded MT (italics) also suggested that there was a high probability that the defaced number was a 6. In the case of the defaced 5, only the Gungsuh (normal) font indicated the best fit was a 5 with the Arial Black (normal, Arial Black (italics) and the Arial Rounded MT (normal) also indicating that there as a high probability that the defaced number was a 5. Based on these results, to get the highest probability of correctly identify a particular serial number, one must be judicious in selecting the fonts to be used in the library. However, it may be difficult to perform this type of selection in practice since in the plastic deformation zone, the numbers can broaden or be somewhat deformed.

III. “Black-Box” or “Blind” Studies Results

A main focus of this grant was to statistically evaluate the capability and viability of using lock-in thermal imaging and subsequent image analysis through matching the PZM and/or RM moments of the score images or phase image with the moments derived from the library (either LIT-MIA *Library Matching* or LIT-ACIP *Classification Matching* methods). These “Black Box” or “Blind” investigations were to be performed based on two criteria:

1. The identity of the defaced serial numbers and location of the serial numbers was unknown, and only revealed after the studies were completed.
2. Recovery of the unknown defaced serial numbers was completed first by thermal imaging and image analysis, and then this same sample was sent to our collaborators at the state forensics lab for serial number recovery by the normal wet chemical methods. The reason for this is it determines the viability of using the thermal image analysis as a preliminary analysis tool, if indeed it is non-destructive. If our collaborators were able to recover the serial numbers after our analysis has been completed, then the non-destructive nature of the thermal method would be verified. The identity of the defaced numbers was unknown until both recovery attempts were completed.

To accomplish this, two types of studies were performed. In one study, which satisfies the first criterion, a serial number recovery study was performed by participation in the 2019 CTS Forensic Testing Program, Test No. 19-5251. A single sample with six defaced serial numbers was provided for this study by CTS and the sample was made of steel. The defacing was done by milling off the metal to a total depth of about 0.5 mm. The identity of the serial number was revealed a few weeks after the serial number reports were received by CTS. The identity of the serial number was: 5 F 3 C 7 K

In a second study, the Idaho State Police Forensic Lab in Coeur d’Alene Idaho was the collaborator and undefaced samples were obtained from Precision Forensics Testing and subsequently defaced by General Products Machine shop in Pocatello. The identity of the numbers was only known to the machine shop personnel and to Scott Pristupa, the materials lab manager in the Chemistry Dept. at Idaho State University. Scott received the materials from Precision Forensics Testing and worked with the machine shop to get them defaced. The Utah Forensic Lab was possibly going to participate, but due to the pandemic they did not. Also, the number of samples had to be reduced to a total of six samples. For this 2nd study three different materials were used: A) Cold Rolled Steel, B) Stainless Steel, and C) Aluminum, and these three samples were defaced by milling to two different depths: 1) 0.08 mm (0.003”) below the point

were the serial numbers disappeared, and 2) 0.30 mm (0.012”) below the point where the serial numbers disappeared. Thus, an example of the labeling of the defaced samples used for this 2nd study was: A1 - the rolled steel sample machined to 0.08 mm below the disappearance point and C4 - the aluminum sample machined to a depth of 0.3 mm below the disappearance point. Table 5 provides the identities of the serial numbers.

Table 5. List of the Sample Material, Deface Depth and Serial Number for 2nd Study

Sample Label	Material	Deface Depth	Serial Number
A1	Rolled Steel	0.08 mm	2632712
B1	Stainless Steel	0.08 mm	7322936
C1	Aluminum	0.08 mm	9163527
A4	Rolled Steel	0.08 mm	2632712
B4	Stainless Steel	0.08 mm	7322936
C4	Aluminum	0.08 mm	9163527

In both Study 1 and Study 2, since the both the position on the sample and the identity of the defaced serial numbers were essentially unknown, a procedure was developed to find one initial character to act as an anchor point from which the other defaced characters could be identified. The procedure used was:

1. Take a series of IR movies from left to right on the sample. Shift the field of view 2-3 mm to the right for each movie. Attempt to keep the movies in a line parallel to the top and bottom edges of the sample. It is also helpful to take a movie of reference numbers if available so the approximate size and spacing of the characters can be determined.
2. Choose a movie from the center of the sample. This assures there is a character in the field of view, assuming the sample was positioned in the center vertically and that the numbers were stamped somewhere near the center of the sample bar.
3. Use software to be able to view a phase plot for the whole movie field of view. Visually look for disturbances in the interference patterns. The goal is to find a horizontal band across the field of view that has spots of disturbances approximately the size of 1 character.
4. Narrow the field of interest with the software to the horizontal band. The row height should be at least the reference character pixel height but could be as much as double the character height. Area width could be the complete width but may be less. Examine the phase image as well as the score plot images. It may be helpful to look at some of the score plot images in black and white. Choose a character sized area to focus on.
5. Run the software for phase image, score plot images and character identification. Check results to see if they match with a visual determination. Refine the window area as needed.
6. Aids to help identify the character are majority vote calculations for a range of score plots, low numbered score images with lowest value for a similarity measure, and lowest sum of all the score plots. The tools work only as well as the accuracy of the designated area of the defaced number. If the number is inaccurately framed, the results will not be accurate. Thus, the procedure used was not totally free from human intervention in finding the best estimate for the defaced number identity.

7. After finding one character, shift the field of interest of the movie either left or right an appropriate amount of space and try to find another character.
8. If step 6 is successful, pick the next movie in the sequence and attempt to find one of the characters previously found. It is important to be looking in the same spot on the sample even though it is a different movie/camera field of view. This can be accomplished with marks on the sample, marks on the paint, or rulers. A plan for translation from movie to movie is important.
9. Work each direction on the sample until the appropriate count of characters are discovered.

Since this procedure is not automated and must be done by the researcher, it can prove to be very time consuming. Also, if a false anchor point on the sample is found, the identification of all of the serial numbers is likely to be invalid since the anchor was not valid. If more information is known about the position of the defaced number, then the procedure is less cumbersome and time consuming. A detailed example of the investigation used for sample B1 is given here. Similar data was generated for the other samples as well.

Based on an initial determination of the anchor position by viewing several thermal imaging movies, the field where the defaced number is thought to be present is divided up into sections which are labeled T U V W X Y and Z and once the data and analysis has been collected the determined serial number values are placed in each of these areas. This is shown below for in Figure 71.

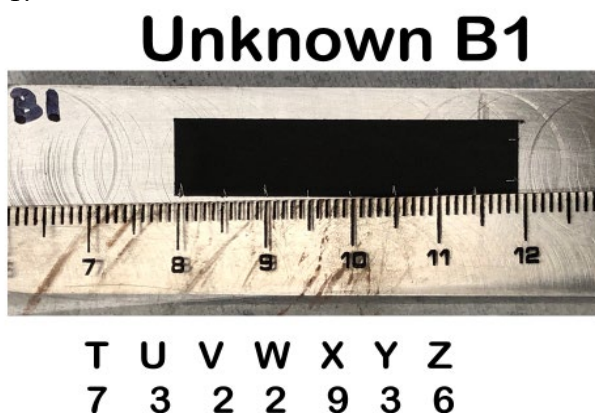


Figure 71. Field Defined for Defaced serial number divided into sections labeled T U V W X Y and Z.

Next the first ten score images are generated from the lock-in thermographic phase images collected from each section. An example of this is shown below in Figure 72 for the T position in Unknown B1. Then score plots undergo preconditioning as described in the previous studies, and the PZM and/or RM moments are generated and compared with those moments from the library as described previously using the Similarity Merits and either the direct Library Matching procedure or the *Classification* procedure. A minimal sum fusion is performed on these merits for each score image. This is shown in Figure 73 for the T position of B1. Note that the labels on the left of the figure s1, s2, etc. are the score image numbers, the numbers at the top of the table are the numerical characters possible for the serial number, and at the bottom of the table is the sum of the minimal sum fusion values for all the score images for each numerical character listed at the top of the table.

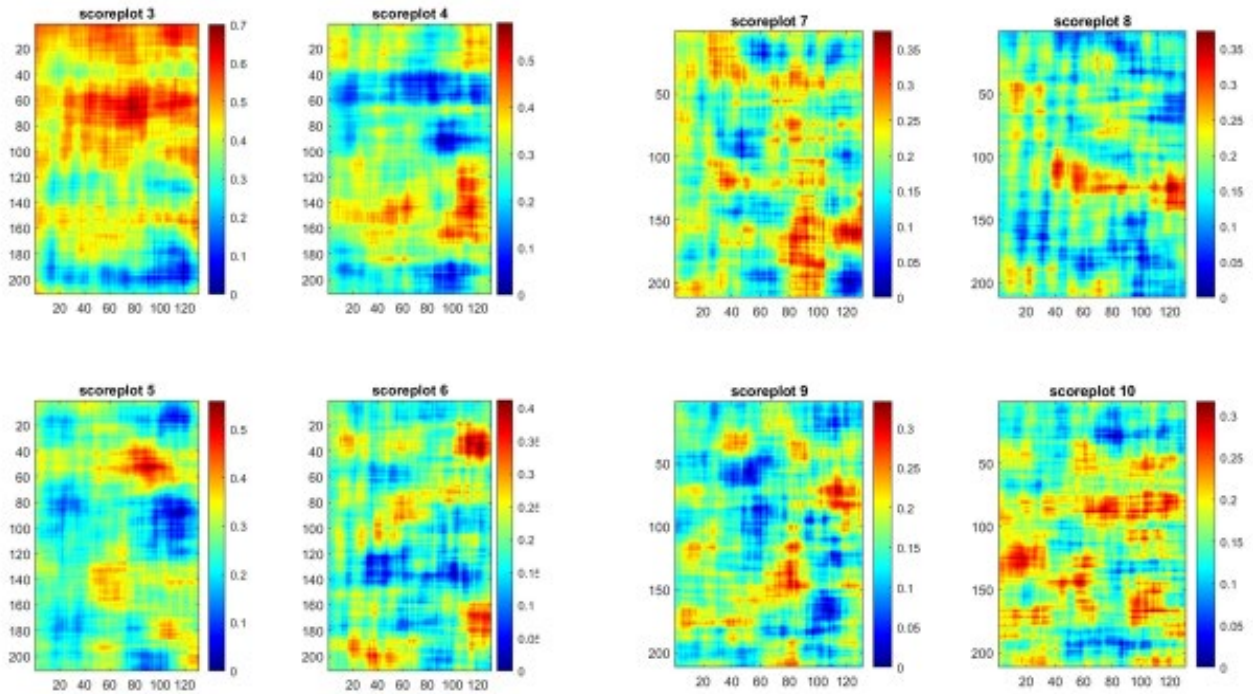


Figure 72. Score plots derived from thermal images of Section T on defaced sample B1.

	0	1	2	3	4	5	6	7	8	9
s1	127	62	96	102	31	88	69	104	44	77
s2	121	4	81	26	11	48	95	46	78	78
s3	94	122	115	110	93	75	26	89	32	28
s4	81	140	112	110	109	86	45	103	35	50
s5	114	45	71	58	39	109	112	31	69	81
s6	55	139	109	78	137	87	33	64	21	84
s7	77	122	81	35	45	57	67	75	33	41
s8	49	126	132	72	121	75	24	90	32	18
s9	38	118	45	77	11	101	46	24	30	20
s10	46	136	85	122	59	110	46	97	24	31
sum	802	1014	927	790	656	836	563	723	398	508

Figure 73. Sum of Fusion Values for each Score Image (s1, s2, s3 ...), for Character Position T, from Library Match of the score images and the overall *sum* of the fusion values. Minimal sum indicates the best match.

Using just the minimal sum value at the bottom of the table to determine the identity of the defaced number represents one computer-based identification of the serial number once the anchor is found. Another method is to look for minimal sum fusion numbers for score image 4, 5, and/or 6 and use that to help identify the defaced number. An example of this is seen in Figure 74.

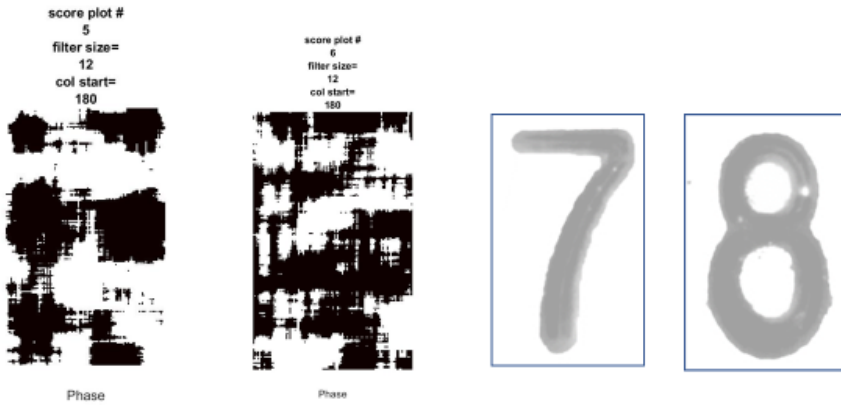


Figure 74. Score images 5 and 6 for Character T. Score image 5 looks mostly like a 7 and Score Image 6 looks mostly like an 8.

Both of these methods were employed to in identifying each character in the defaced samples. Thus, even though the overall sum of the fusion values for each numerical character is lowest for an 8 (value is 398), since score image 5 has the lowest fusion of merit values if the defaced character's identity is a 7 (value of 31). So defaced character T is likely a 7 or an 8.

In another example, for the defaced number in position Z, score images from one set of thermal mages are shown in Figure 75 and the merit value sum fusion values are given in Figure 76.

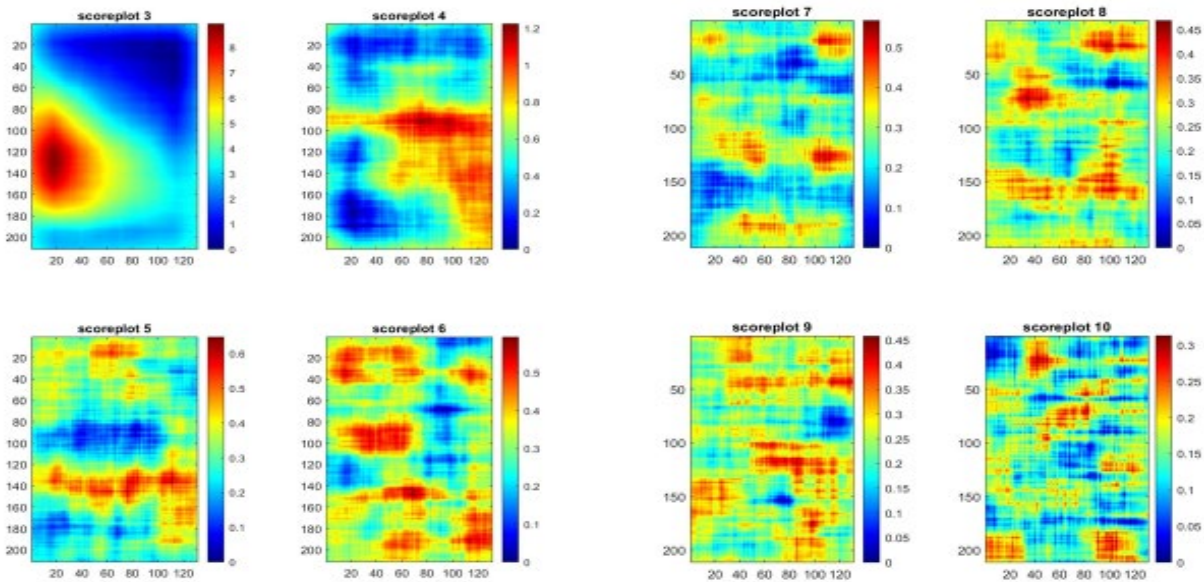


Figure 75. Score plots derived from thermal images of Section Z on defaced sample B1.

	0	1	2	3	4	5	6	7	8	9
s1	127	64	99	103	35	91	73	99	49	79
s2	92	73	85	23	4	78	47	111	29	49
s3	121	111	106	116	86	81	59	89	65	77
s4	91	85	110	57	30	62	51	118	21	41
s5	83	66	78	76	26	99	68	36	52	84
s6	106	101	108	114	118	89	50	67	80	105
s7	29	139	111	90	123	35	12	109	44	5
s8	78	132	74	65	92	36	27	102	20	77
s9	77	132	77	41	63	49	60	114	26	53
s10	42	140	114	100	122	79	22	125	61	70
sum	846	1043	962	785	699	699	469	970	447	640

Figure 76. Sum of Fusion Values for each Score Image (s1, s2, s3 ...), for Character Position Z, from Library Match of the score images and the overall *sum* of the fusion values. Minimal sum indicates the best match.

For character position Z the overall sum is essentially the same for character 6, and character 8, (469 and 447) respectively. Analysis of the individual score image fusion numbers indicates the number could be 8 (lowest fusion for score image 7) or 6 (lowest fusion for score image 6). These score images are given below in Figure 77. Visually, the left side seems heavier than the right favoring a 6.

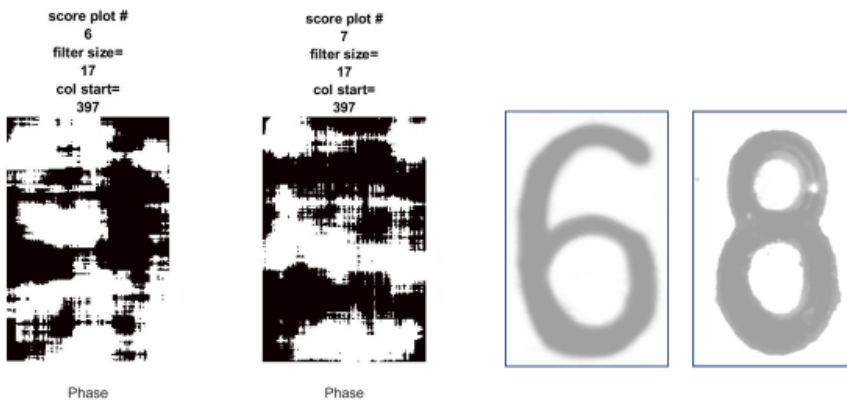


Figure 77. Score images 6 and 7 for Character Z. Score image 6 looks mostly like a 6 and Score Image 7 looks mostly like an 8.

A similar analysis was performed on the other sections of unknown sample B1, and once an anchor character was found for unknown A1 and C1, their surface was sectioned and analyzed in the same way to determine the identities of all the defaced serial characters for these three samples. Ultimately the values reported for the defaced serial number were determined from weighing the overall fusion summed over all the score images compared with the library, and the individual score image merit values for the character of interest. No anchor character could be found for the more deeply defaced numbers, and thus the serial numbers on samples A4, B4, and C4 could not be recovered by the thermal imaging method.

Once the lock-in thermal imaging was completed, the same samples were then given to Stuart Jacobsen at the Idaho State Police Forensic Lab in Coeur d'Alene Idaho. The police lab there performed the standard wet chemical methods to recover the defaced serial numbers. It

was possible for them to analyze the same samples since the thermal imaging technique should not damage the samples. The results of the serial number recovery from both the lock-in thermal imaging determination and the Idaho Forensic Lab are given in Table 5 along with the true values.

Table 6. Comparison of the Serial Number Recovery Results from the Thermal Imaging and Wet Chemical Method

Sample Label	Material	Deface Depth	Thermal Imaging	State Police Wet Chemical	True Serial #
A1	Rolled Steel	0.08 mm	9846853	2638712	2632712
B1	Stainless Steel	0.08 mm	7322936	7322936	7322936
C1	Aluminum	0.08 mm	5648947	91xx5(2/8)7	9163527
A4	Rolled Steel	0.08 mm	indeterminate	(8/2)xxx712	2632712
B4	Stainless Steel	0.08 mm	indeterminate	7322936	7322936
C4	Aluminum	0.08 mm	indeterminate	indeterminate	9163527

Note that the thermal imaging technique was able to correctly identify a total of only 8 characters out of a possible 42 characters. The wet chemical method was able to correctly identify 29. Said another way, the thermal imaging method had a 19% success rate and the wet chemical method had a 69% success rate. It should be noted that based on the results of the Idaho State Police Lab, analysis of the unknown samples first by the thermal imaging lab, did not appear to seriously impede their recovery by the wet chemical methods.

This type of thermal imaging analysis was performed with the July 2019 CTS steel sample using similar heating and cycling parameters. It proved very difficult to find any character that could be confidently assigned as an anchor character using the phase image technique described above in Figure 16. Eventually in movie, a phase image appeared to show a character present although it was not as readily identifiable in other movies take of the same area. Based on this anchor position, the imaging in areas where characters to the right and left should appear was accomplished, calculating fusion sums for particular score images, fusion sums for all 15 score images, and visual inspection of what were assumed to be the best score images. The restored serial number we submitted to CTS based on this information was:

3 E 4 2 B 8

and the true identity of the defaced characters was:

5 F 3 C 7 K

In this study, the thermal imaging method did not provide even one match to the true identity of the characters for this particular sample. As noted above, it was very difficult to identify an anchor character, and identification of each subsequent character was also difficult. Possible problems with the methodology we used include: failure to correct for the large difference in the thermal conductivity of the samples, failure to restrict the matching library to fonts more consistent with the fonts stamped into the testing samples, failure to perform enough sanding to smooth out the variations in the samples leftover from the defacing before applying the black paint, noise introduced into the system from pulsing circuit drift, lack of consistent laser heating and heating profile.

IV. Summary

In summary several aspects of the thermal imaging analysis were studied in an attempt to determine the best practice to use when implementing the method. In particular the following aspects of the thermal imaging method were studied: Surface Prep and Recovery Depth, Score Image Contribution, Best Use of Similarity Measures, Libraries and Computerized Matching Algorithms, and “Black-Box” or “Blind” Studies Results.

The studies on the surface preparation indicated that it was important to polish the samples to the degree that significant lines or swirls in the material were reduced significantly. This could be accomplished by sanding the sample with increasing grit numbers starting at about 400 and a final polish with 1200 or higher grit paper. Additionally, the emissivity and heat absorption of the sample can be changed by painting the surface. Studies showed that the number of coats of paint on the surface decreased the recovery if there were more than two coats. Typically, one coat of black paint applied with the doctor blade method gave better serial number recovery. The use of black electrical was also studied as an alternative to black paint to change the absorption and emissivity of the sample. Results with the electrical tape were promising, and an added benefit was electrical tape applied to undefaced serial numbers on a sample seemed to enable determination of the correct lock-in frequency to use to produce the lock-in phase images.

Experiments were also performed to determine the depth to which the serial number samples can be defaced before the serial number is no longer recoverable. These studies suggested, that with a ~ 2 W of laser heating power, serial number recovery below a defacing depth of about 0.5 mm was not possible. This was judged largely by the difficulty encountered in correctly identifying the defaced serial numbers on metals that were defaced in a stepped fashion.

Studies on the score image contribution were largely aimed at determining if a single consistent score image could be matched with the library using pseudo-Zernicke moments of each and a fusion of the similarity merits. Ideally a low score image like PC4-PC7 might look consistently contain an image of the defaced serial number, and if so it could be consistently used in the matching routine. In past studies, from the previous grant, all of the score images were used in matching to the library. The results from these studies showed that although often a score image like PC4 or PC7 contains an image that provides a good match to the defaced serial number, that score image does not always provide a good match for a different sample. For a different sample a different score image like PC5 might provide a better match. Thus, it is likely better to use all of the score images in the matching routine, or if a single score image is used, it should visually look very close to a particular number.

In the studies of the score image contribution, the effect of using different cycles to produce the score image was also studied. Here for instance, 60 heating cycles were used to produce a particular score image, say PC4, versus using only the last 20 heating cycle to produce the score image, PC4. Visually, for an undefaced sample, it appeared that PC4 contained similar information and matched well to a 2, but for an undefaced sample, picking different heating cycles changed PC4 visually and the matching results changed as well. Typically, the best matches were found when a large number of heating cycles was used to produce the score image.

The final study for the score image contribution was to not use the score image at all, and to simply use the phase image derived from the lock-in thermography. Here the best lock-in frequency was determined from the use of the black electrical tape covering an undefaced character, and then the phase image was calculated from a heating cycle. To match the phase image with the library images, a different match procedure was developed which used *Classification* rather than directly library matching as in the previous grant. Direct use of the lock-in phase images and comparison to the library characters with the *Classification* method appeared to correctly identify both undefaced and deface serial numbers, at least on samples where the exact location of the sample is known. This serial recovery method of using the phase images with the *Classification* library comparison routine was largely developed by the MS student, Anit Gurung, working on the project and is called the ACIP method. Overall this last study using just the phase image suggests that score images may not be necessary for the library matching.

Studies of the Similarity Merits focused on the effect of dilation of the score images or phase images on the similarity merits and on their comparison with the library. Also studied was the effect of using rotationally variant vs rotationally invariant moments to calculate the moments and merit values for library matching. With regard to dilation, changing the object proportion can have a large effect on the similarity merits and on the library match. Changing the object proportion from 35% to 50% and/or 65% resulted often in a significant change in the similarity merit values and their sum fusion, and often increase in correct identification of the defaced character. In some cases lowering the object proportion increased the success of correctly identifying the character.

Some alpha-numeric characters like a 6 and a 9 can look like and be identified as one another if the moments used to describe these numbers are rotationally invariant. Zernicke moments and pseudo-Zernicke moments (PZM) are rotationally invariant. However, for serial number identification, the rotational orientation is fixed, and so a rotationally variant set of moments would likely represent the serial number characters more effectively and would provide for better similarity merits and an increased chance of getting a correct match. The Radial moments (RM) have the property of being rotationally variant. A comparison of the use of the PZM moments and the RM moments showed that more favorable similarity merits and an increase in the correct serial number identification could be realized when RM moments were used instead of PZM moments in comparing lock-in thermal images with the library.

Studies performed also involved investigating how the comparison by similarity measures and fusion rules was affected by using one font in the numerical library for several common fonts. For the previous grant we used 10 font types in the numerical comparison library, and here we investigated how the identification of the defaced number is affected by using only a single font. Based on these results, it appears that some fonts contribute more to the correct identification of the defaced serial number than others. Based on these results, to get the highest probability of correctly identify a particular serial number, one must be careful in selecting the fonts to be used in the library. However, it may be difficult to perform this type of

selection in practice since in the plastic deformation zone, the numbers can broaden or be somewhat deformed.

Perhaps the most important results from these studies were the “Blind Tests” or “Black-box Studies” performed in collaboration with the Idaho State Police Lab. Here unknown samples were first analyzed with the lock-in thermal imaging method, and then the same samples were sent to the Police lab for analysis by wet chemical methods. These studies served two purposes. One purpose was to test the thermal imaging method against the standard wet chemical method. The other was to determine if the thermal imaging method had any affect on the serial recovery of the numbers by the standard wet chemical method. The thermal imaging technique only had a 19% recovery rate as compared with a 69% success rate through the wet chemical method. The thermal image technique also had difficulty recovering the serial numbers from the 2019 CTS Forensics Testing Program. None of the serial characters were correctly identified, although when similar testing was performed on an obsolete CTS Forensic unknown sample, several of the numbers were identified.

Overall, the results from the Black-box studies appear to reveal a shortcoming of recovering defaced serial numbers from defaced samples where there is minimal or no idea of the position of the defaced numbers on the sample. The procedure to find that first character to act as an anchor point is an arduous task and subject to large pitfalls if a false anchor point is identified. If the position of the characters are known to a large degree, then the thermal imaging method would likely be more viable as a tool or at least a preliminary tool for serial number recovery, since it is non-destructive to the sample as was shown in these investigations. Lastly, further studies using the *Classification* methodology for matching the phase or score images with the library may benefit the use of thermal imaging.

V. REFERENCES

1. Ikwulono Unobe, Lisa Lau, John Kalivas, Rene Rodriguez and Andrew Sorensen, "Restoration of defaced serial numbers using lock-in infrared thermography (Part I)", *Journal of Spectral Imaging*, (2019) 8
2. Ikwulono Unobe, Lisa Lau, John Kalivas, Rene Rodriguez and Andrew Sorensen, "Restoration of defaced serial numbers using lock-in infrared thermography (Part II)", *Journal of Spectral Imaging*, (2019) 8
3. Suykens, J. A., & Vandewalle, J. (1999). Least squares support vector machine classifiers. *Neural processing letters*, 9(3), 293-300.
4. Chua, L. O., & Yang, L. (1988). Cellular neural networks: Theory. *IEEE Transactions on circuits and systems*, 35(10), 1257-1272.
5. Yegnanarayana, B. (2009). *Artificial neural networks*. PHI Learning Pvt. Ltd.
6. Khotanzad, A., & Hong, Y. H. (1990). Invariant image recognition by Zernike moments. *IEEE Transactions on pattern analysis and machine intelligence*, 12(5), 489-497.
7. Pang, Y. H., BJ, A. T., & CL, D. N. (2005). Enhanced pseudo Zernike moments in face recognition. *IEICE Electronics Express*, 2(3), 70-75.
8. PLS-DA. (n.d.). from June 22, 2020, at <https://imdevsoftware.wordpress.com/tag/pls-da/>
9. Ali, A. (2019, November 24). K-Nearest Neighbor with Practical Implementation. Retrieved June 22, 2020, from <https://medium.com/machine-learning-researcher/k-nearest-neighbors-in-machine-learning-e794014abd2a>

VI. DISSEMINATION OF RESEARCH FINDINGS

1. Prof Kalivas presented a talk at Pittcon on the Defaced Serial Number Recovery by Thermal Imaging in Philadelphia, PA in March 2019 for session sponsored by NIJ (National Institute of Justice)
2. Professor Rodriguez gave a webinar titled " RESTORATION OF DEFACED SERIAL NUMBERS USING INFRARED THERMAL IMAGING" as part of the Research and Development Webinar Series through the Forensic Technology Center of Excellence (FTCoE), a program of the National Institute of Justice (NIJ) on Feb. 26, 2019.

3. The group provided an abstract for the LEAP Newsletter in Feb 2019 with title "Development of a Non-destructive Technique for the Restoration of Defaced Serial Numbers"
4. Lisa Lau gave an oral presentation at the Idaho Academy of Science and Engineering Meeting in Boise Idaho in April 2019 with title " Thermal Imaging Method for Recovering Defaced Stamped and Laser Engraved Serial Numbers"
5. Two papers were published on work from the previous grant.
 - a. [Journal of Spectral Imaging](#), [Volume 8](#) Article ID a19 (2019)
Restoration of defaced serial numbers using lock-in infrared thermography (Part I)
Ikwulono Unobe, Lisa Lau, John Kalivas, Rene Rodriguez and Andrew Sorensen
 - b. [Journal of Spectral Imaging](#), [Volume 8](#) Article ID a20 (2019)
Restoration of defaced serial numbers using lock-in infrared thermography (Part II)
Ikwulono Unobe, Lisa Lau, John Kalivas, Rene Rodriguez and Andrew Sorensen
6. US Patent 10/657,413 entitled, Restoration of defaced markings using lock-in infrared thermography, issued on May 19, 2020

Appendix 1 Similarity Merits

i. Correlation Coefficient:

$$CC = \frac{S_{12}}{S_1 S_2}$$

Where,

S_1 and S_2 = the standard deviations of variables (vectors) 1 and 2 respectively

S_{12} = covariance of variables

ii. Euclidean Distance:

$$1-ED = 1 - \sqrt{(x_1 - x_2)(x_1 - x_2)^T}$$

Where,

x_1 and x_2 = vectors representing Zernike moments for a pristine number from the library and a score image from the recovered numbers respectively.

iii. Angle between vectors:

$$\cos \theta = \frac{|x_1^T x_2|}{\|x_1\| \|x_2\|}$$

iv. Determinant:

$$Det = 1 - \left| \begin{pmatrix} x_1^T \\ x_2^T \end{pmatrix} (x_1 \quad x_2) \right| = (\|x_1\| \|x_2\| \sin \theta_1)^2$$

v. Procrustes Analysis:

$$x_1 = x_2 F_{21}$$

$$F_{21} = (x_2 x_2^T)^+ (x_2 x_1^T)$$

$$F_{22} = (x_2 x_2^T)^+ (x_2 x_2^T)$$

$$F = \|F_{21} - F_{22}\|_F$$

Where,

F = a transformation matrix necessary to make \mathbf{x}_2 most similar to \mathbf{x}_1

$(\mathbf{x}_2\mathbf{x}_2^T)^+$ = pseudoinverse of $\mathbf{x}_2\mathbf{x}_2^T$

$\|F_{21} - F_{22}\|_F$ = the Frobenius norm for the matrix difference between the two transformation matrices F_{21} and F_{22}

vi. Constrained Procrustes Analysis

$$\mathbf{x}_2^T \mathbf{x}_1 = \mathbf{U}_{21} \Sigma_{21} \mathbf{V}_{21}^T$$

$$\rho_{21} = \frac{\text{tr}(\Sigma_{21})}{\text{tr}(\mathbf{x}_2\mathbf{x}_2^T)}$$

$$\mathbf{H}_{21} = \mathbf{U}_{21} \mathbf{V}_{21}^T$$

$$\rho = \|\rho_{21} - \rho_{22}\|_{Frob}$$

$$H = \|\mathbf{H}_{21} - \mathbf{H}_{22}\|_{Frob}$$

Where,

$$\mathbf{X} = \mathbf{x}_2^T \mathbf{x}_1$$

\mathbf{U} = eigenvectors of matrix $\mathbf{X}\mathbf{X}^T$

Σ = diagonal matrix of singular values

\mathbf{V} = loading matrix = eigenvectors of matrix $\mathbf{X}^T\mathbf{X}$

vii. Mahalanobis Distance:

$$\mathbf{C}_1 = \mathbf{x}_1\mathbf{x}_1^T$$

$$MD = \sqrt{(\mathbf{x}_2 - \mathbf{x}_1)^T \mathbf{C}_1^+ (\mathbf{x}_2 - \mathbf{x}_1)}$$

viii. Pooled Mahalanobis Distance:

$$\mathbf{S}_1 = \mathbf{x}_1\mathbf{x}_1^T$$

$$\mathbf{S}_2 = \mathbf{x}_2 \mathbf{x}_2^T$$

$$\mathbf{C} = \frac{\mathbf{S}_1 + \mathbf{S}_2}{2}$$

$$PMD = \sqrt{(\mathbf{x}_1 - \mathbf{x}_2)^T \mathbf{C} (\mathbf{x}_1 - \mathbf{x}_2)}$$

ix. Bartlett Statistics:

$$\mathbf{S}_1 = \mathbf{x}_1 \mathbf{x}_1^T$$

$$\mathbf{S}_2 = \mathbf{x}_2 \mathbf{x}_2^T$$

$$\mathbf{S} = \frac{\mathbf{S}_1 + \mathbf{S}_2}{2}$$

$$\nu = \left(\frac{2n^2 + 3n - 1}{6(n+1)} \left[\frac{-1}{m_1 + m_2} \right] \right)$$

$$c = \nu [(m_1) \ln(|\mathbf{S}_1^+ \mathbf{S}|) + (m_2) \ln(|\mathbf{S}_2^+ \mathbf{S}|)]$$

$$BS = \exp\left(\frac{-c}{m_1 + m_2}\right)$$

Where,

n = the number of variables

m_1 and m_2 = the number of samples in each dataset being compared. In this study, only two vectors are being compared so m_1 and m_2 are equal to one.